의학 박사 학위논문

토끼 VX2 간암 모델에서 다중지표 자기공명영상을 이용한 혈관차단제(CKD-516)의 치료 효과 평가

2013년 2월

서울대학교 대학원

의학과 영상의학 전공

주 이 진

토끼 VX2 간암 모델에서 다중지표 자기공명영상을 이용한
혈관차단제(CKD-516)의 치료 효과 평가

2013년

주이진

의학 박사 학위논문

토끼 VX2 간암 모델에서 다중지표 자기공명영상을 이용한 혈관차단제(CKD-516)의 치료 효과 평가

2013년 2월

서울대학교 대학원

의학과 영상의학 전공

주 이 진

Doctoral Thesis

Multiparametric MRI for Monitoring the Therapeutic Efficacy of a Vascular Disrupting Agent (CKD-516) in Rabbit VX2 Liver Tumors

February 2013

The Graduate School, Seoul National University

Medicine – Radiology

Ijin Joo

토끼 VX2 간암 모델에서 다중지표 자기공명영상을 이용한 혈관차단제(CKD-516)의 치료 효과 평가

지도 교수 이 정 민

이 논문을 의학박사 학위논문으로 제출함
2012년 10월

서울대학교 대학원
의학과 영상의학 전공
주 이 진

주이진의 의학박사 학위논문을 인준함
2012년 12월

위 원 장 _____ (인)
부위원장 _____ (인)
위 원 _____ (인)
위 원 _____ (인)
위 원 _____ (인)

학위논문 원문제공 서비스에 대한 동의서

본인의 학위논문에 대하여 서울대학교가 아래와 같이 학위논문 제공하는 것에 동의합니다.

1. 동의사항
① 본인의 논문을 보존이나 인터넷 등을 통한 온라인 서비스 목적으로 복제할 경우 저작물의 내용을 변경하지 않는 범위 내에서의 복제를 허용합니다.

② 본인의 논문을 디지털화하여 인터넷 등 정보통신망을 통한 논문의 일부 또는 전부의 복제. 배포 및 전송 시 무료로 제공하는 것에 동의합니다.

2. 개인(저작자)의 의무
본 논문의 저작권을 타인에게 양도하거나 또는 출판을 허락하는 등 동의 내용을 변경하고자 할 때는 소속대학(원)에 공개의 유보 또는 해지를 즉시 통보하겠습니다.

3. 서울대학교의 의무
① 서울대학교는 본 논문을 외부에 제공할 경우 저작권 보호장치(DRM)를 사용하여야 합니다.

② 서울대학교는 본 논문에 대한 공개의 유보나 해지 신청 시 즉시 처리해야 합니다.

논문제목 : 토끼 VX2 간암 모델에서 다중지표 자기공명영상을 이용한 혈관차단제(CKD-516)의 치료 효과 평가

학위구분 : **석사** □ · **박사** ■
학 과 : 의학과
학 번 : 2011-30580
연 락 처 :
저 작 자 : 주이진 (인)

제 출 일 : 2013 년 2 월 3 일

서울대학교총장 귀하

ABSTRACT

Objectives: To evaluate the diagnostic value of multiparametric MRI, including intravoxel incoherent motion (IVIM) diffusion-weighted imaging (DWI) and dynamic contrast enhanced (DCE) MRI, in the quantitative assessment of the therapeutic efficacy of a vascular disrupting agent (VDA) (CKD-516) in rabbit VX2 liver tumors

Methods: In twenty-one VX2 liver tumor-bearing rabbits (15 in the treated group and 6 in the control group), IVIM-DWIs using 12 *b* values and DCE-MRIs were performed at a 3T scanner before and 4 hours, 24 hours, 3 days, and 7 days after CKD-516 administration. IVIM-DWI parameters including the apparent diffusion coefficient (ADC), true diffusion coefficient (*D*), pseudo-diffusion coefficient (D^*), perfusion fraction (*f*), and blood flow-related parameter (fD^*), and DCE-MR parameters including the volume transfer coefficient (K^{trans}) and initial area under the gadolinium concentration-time curve until 60 seconds (iAUC) of tumors were compared between the control and treated groups as well as among different time points. Correlation between changes in tumor size and IVIM-DWI and DCE-MR parameters was analyzed to determine which MR parameters could be used as predictors for tumor response. Correlation analysis between

parameters derived from IVIM-DWI and DCE-MRI was performed.

Results: The treated group showed a significantly larger increase in ADC at 24 hours, a decrease of D^* and fD^* at 4 hours, and a decrease of f, K^{trans}, and iAUC at 4 hours and 24 hours, than the control group ($P<0.05$). In addition, compared to baseline values, D^*, f, fD^*, K^{trans}, and iAUC of the treated group significantly decreased at 4 hours and then, recovered at 24 hours or 3 days, and D significantly increased at 24 hours ($P<0.005$). The greater decrease in f and fD^* at 4 hours correlated with the smaller increase in tumor size during the 7 days (rho=0.53 and 0.65, P=0.04 and 0.009, respectively). There was no significant correlation between measured parameters of IVIM-DWI and DCE-MRI ($P>0.05$), however, a positive correlation was observed between the relative percentage changes in fD^* and K^{trans} at 4 hours (rho=0.54, P=0.04).

Conclusion: The therapeutic effect induced by VDA can be effectively evaluated using IVIM-DWI and DCE-MRI, and f and fD^* derived from IVIM-DWI can be early predictive indicators for tumor response.

Keywords: intravoxel incoherent motion diffusion-weighted MRI, dynamic-contrast enhanced MRI, vascular disrupting agent, CKD-516, liver cancer,

VX2 carcinoma

Student Number: 2011-30580

목 차

List of Tables

List of Figures

.

List of Abbreviations

VDA = vascular disrupting agent

IVIM = intravoxel incoherent motion

ADC = apparent diffusion coefficient

D = true diffusion coefficient

D^* = pseudo-diffusion coefficient

f = perfusion fraction

fD^* = blood flow-related parameter

DCE = dynamic contrast enhanced

K^{trans} = volume transfer coefficient

iAUC = initial area under the gadolinium concentration-time curve until 60 seconds

INTRODUCTION

Angiogenesis is an essential process of tumor growth in which tumor vessels supply oxygen as well as other nutrients to the tumor (1, 2). However, new vessels arising from tumor angiogenesis are structurally and functionally abnormal, and differ from normal vasculature. Thus, these newly formed tumor vessels can be used as valuable selective targets for anticancer therapy. There are currently several kinds of vascular targeting agents being developed and used for the treatment of malignant tumors both clinically or in phase II or III clinical trials (1, 2), and they can be classified into either anti-angiogenic drugs which inhibit new vessel formation or vascular disrupting agents (VDAs) which destroy established tumor vessels, subsequently causing tumor ischemia and necrosis (3). As a noninvasive and quantitative method of monitoring the treatment efficacy of these vascular targeting agents would be ideal, tumor size change on imaging studies has been widely used as a standard endpoint in evaluating tumor response to anticancer therapy. However, for the monitoring of vascular targeting agents, size measurement may be insensitive or delayed chronologically and thus cannot be relied upon to reflect the therapeutic

effect accurately and promptly (4). Thus, several kinds of functional imaging techniques have been evaluated as more accurate alternatives (5-10). These include perfusion imaging studies using dynamic contrast-enhanced (DCE) ultrasound/CT/MRI which can allow assessment of the tumor microvasculature, and diffusion-weighted MRI (DWI) in which information of tumor cellularity and necrosis can be obtained.

Considering that VDAs can induce cell death and necrosis through the destruction of established tumor vessels, evaluation of both microperfusion characteristics and cellular necrosis might be an idealistic way to evaluate the therapeutic response of VDAs. In this aspect of VDA treatment monitoring, multiparametric MRI can provide variable imaging biomarkers of not only morphologic characteristics but also functional characteristics; Conventional T2-weighted and T1-weighted images offer morphologic characteristics such as tumor size, DCE-MRI derived parameters give information regarding hemodynamic changes in the tumor, and DWI provides information of tumor cellularity and necrosis (11).

Recently, DCE-MRI has been increasingly used in the clinical trials of anti-angiogenic drugs as a non-invasive method to quantitatively show the acute changes in tumor perfusion induced by anti-angiogenic treatment

(12). However, for monitoring the therapeutic effect of VDAs, only a few studies have demonstrated the usefulness of DCE-MRI. It has been suggested that the appropriate timing of imaging studies would be important for monitoring VDA treatments because the effects of VDAs are typically seen within hours and may disappear within 24 hours, while the effects of anti-angiogenic drugs appear within days to weeks (10, 13). CKD-516, a novel small-molecule VDA, is an anti-tubulin drug which has dual action mechanisms of: 1) disrupting blood flow selectively in the tumor resulting in hypoxia and necrosis, and 2) arresting the cell cycle resulting in apoptosis (14). The serial change in tumor perfusion induced by this new VDA, CKD-516 has not been evaluated in an *in vivo* study which can be quantitatively measured by DCE-MRI. In addition, an appropriate imaging schedule has not yet been established.

Intravoxel incoherent motion (IVIM) DWI initially described by Le Bihan et al (15) can separately estimate microcirculation in the capillaries as well as molecular diffusion using bi-exponential fitting of the DWI data from multiple *b* values (16). Furthermore, as IVIM-DWI does not require any contrast medium, this method could be applicable within a short time interval for evaluation of therapeutic response. I surmised that IVIM-derived

parameters might be useful to monitor the micro-environmental changes of the tumor after administration of VDAs, as VDAs would affect the tumor vasculature and result in necrosis of the tumor (17, 18). Until now, there have been a few studies on the use of IVIM-DWI for evaluation of anti-angiogenic drugs (17), however, there have been no previous studies which have evaluated the diagnostic value of IVIM-DWI for the evaluation of the therapeutic effect of VDAs.

Therefore, this study was attempted to evaluate the feasibility of multiparametric MRI including IVIM-DWI and DCE-MRI for the quantitative assessment of the therapeutic efficacy of CKD-516 in a Rabbit VX2 liver tumor model.

MATERIALS AND METHODS

Animal Model

This study was approved by the Animal Care and Use Committee of Seoul National University Hospital (IACUC No. 11-0259 and 12-0245). Twenty-nine male New Zealand White rabbits weighing between 2.5 to 3.5 kg each were used. Prior to tumor implantation, animals were sedated with an intravenous injection of 5 mg/kg of a 1:1 combination of tiletamine hydrochloride and zolazepam (Zoletil; Virbac, Carros, France) and xylazine hydrochloride (Rompun 2%; Bayer Korea, Seoul, Korea). Through a midline abdominal incision, the left lobe of the liver was exposed and an approximately 5 mm tunnel was made in the subcapsular area of the left lobe of the liver. Afterwards, approximately 1 mm^3 of minced pieces of harvested fresh VX2 carcinoma tissue were locally implanted into the liver through the tunnel. VX2 liver tumors were incubated for 12 to 14 days after the tumor implantation prior to baseline imaging.

Vascular Disrupting Agent (CKD-516) Preparation

CKD-516 (Chong Kun Dang Pharm, Seoul, Korea) was dissolved in 5 mL

of saline at a dose of 5, 9, or 12 mg/m^2 body surface area. For the treated group, a CKD-516 solution was administered by slow intravenous injection over 5 minutes via the auricular vein.

Experimental Protocol

Twelve to fourteen days after tumor implantation, twenty-nine tumor-carrying rabbits were randomly divided and placed into the control group (n=6) (G1) and CKD-516 treated groups at different dosage regimens of 5, 9, and 12 mg/m^2 (n=5, 9, and 9) (G2, G3, and G4). Immediately after baseline MR scanning, CKD-516 was administered to the treated group (n=23). For each subject both in the control and treated groups, follow-up MR imaging studies were performed at 4 hours, 24 hours, 3 days, and 7 days after the baseline imaging study. Among the 29 rabbits, eight rabbits in the treated group died during the experimental period: four in G3 and the other four in G4. Therefore, 21 rabbits which survived until 7 day follow-up were finally included in this study: 6 in the control group (G1) and 15 in the treated group (5 in G2, 5 in G3, and 5 in G4).

MR Image Acquisition

MR imaging examinations were performed using a 3T MR imaging system (Magnetom Trio, Siemens Medical Solutions, Erlangen, Germany) using a human knee coil. Prior to each MRI scanning, anesthesia was induced as described above. MR examination was performed in the supine position and included the entire liver. After routine localization images, transverse T2-weighted fast spin echo images (TR=4100 msec, TE=87 msec, slice thickness=3 mm, matrix=512x358) and T1-weighted images using a gradient echo (GRE) sequence (TR=3.5 msec, TE=1.5 msec, slice thickness=3 mm, matrix=128x128) were acquired.

Subsequently, IVIM –DW images were obtained using a free-breathing, single-shot echo-planar imaging pulse sequence with diffusion gradients applied in three orthogonal directions using the following parameters: TR=2700 msec, TE=63 msec, slice thickness=3 mm, number of excitation (NEX)=8, FOV=14x14 cm, matrix=128x128, and multiple b values=0, 10, 20, 30, 40, 50, 75, 100, 150, 200, 400, 800 sec/mm^2. The acquisition time was 12 minutes 20 seconds for IVIM-DWI. The spectral selection attenuated inversion (SPAIR) technique was used for fat suppression.

For T1 mapping, unenhanced T1-weighted volumetric interpolated breath

hold examination (VIBE) images were acquired at each of the three flip angles using following parameters: TR=3.9 msec, TE=1.4 msec, flip angles (α=2°, 8° and 15°), slice thickness=3 mm, NEX=4, FOV=14x14 cm, matrix=128x128, number of slices=20. Then, DCE-MRI using free-breathing, radial 3D VIBE with k-space-weighted image contrast (KWIC) reconstruction was performed after an intravenous bolus injection of 0.1mmol/kg of gadoteric acid (Dotarem, Guerbet, Paris, France). The parameters were TR=3.5 msec, TE=1.5 msec, flip angle=11°, slice thickness=3 mm, NEX=2, receiver bandwidth=780 Hz/pixel, FOV=14x14 cm, matrix=128x128, number of slices=20. The DCE-MRI was continuously scanned 15 times during 180 seconds.

Image Analysis

IVIM Parametric Map Acquisition

DWI data was post-processed using a vendor supplied prototype software program (Siemens Healthcare, Erlangen, Germany) to extract the apparent diffusion coefficient (ADC) and IVIM parameters including the true diffusion coefficient (*D*), pseudo-diffusion coefficient (D^*), and perfusion fraction (*f*). ADC values were automatically calculated using all *b* values

with a mono-exponential fit. According to the IVIM concept, the relative signal intensity is given by: $\mathbf{SI/SI_0} = (\mathbf{1} - \boldsymbol{f}) \times \mathbf{exp}(-\mathbf{b}\boldsymbol{D}) + \boldsymbol{f} \times \mathbf{exp}(-\mathbf{b}\boldsymbol{D}^*)$, in which SI_0 is the mean signal intensity of the region of interest (ROI) for *b* value=0, and SI is signal intensity for the higher *b* value. Using this equation, *D*, D^*, and *f* values were calculated using a non-linear bi-exponential fit (19). Four parametric maps of ADC, *D*, D^*, and *f* were created on a pixel-by-pixel basis for each case (Fig. 1).

DCE-MR Parametric Map Acquisition

According to the consensus opinion on DCE-MRI in assessing vascular targeting agents in clinical trials (10, 20), we measured the two most commonly used perfusion-related DCE-MR parameters including voxel-wise perfusion maps of volume transfer coefficient (K^{trans}) and initial area under the gadolinium concentration-time curve until 60 seconds (iAUC) to evaluate the perfusion change induced by CKD-516. Using DCE-MR images, parameteric maps of K^{trans} and iAUC were generated using a post-processing software program (Tissue4D, Siemens Medical Solutions, Erlangen, Germany) based on the Tofts model (Fig. 2) (21, 22).

Quantitative Measurement

For quantitative image analysis, one blinded radiologist (I.J.) with 5 years of experience in MR imaging measured the tumor size and diffusion-weighted MR values. Response to treatment was determined by the change in tumor size defined as the longest diameter measured on axial T2-weighted images. For each subject, percentage change in tumor size between baseline and 7 day follow-up was calculated using the following equation: $\mathbf{Size\ change}\ (\%) = (\mathbf{LD_{7days}} - \mathbf{LD_{baseline}})/\mathbf{LD_{baseline}} \times \mathbf{100},$ in which LD is the longest diameter of the tumor. To evaluate inter-observer variability for size measurement on T2-weighted images, all cases of 7 day follow-up were also measured by one other blinded radiologist (E.S.L.).

For each time point, diffusion- weighted MR values including ADC and IVIM parameters and DCE-MR values including K^{trans} and iAUC of the tumor were measured using an operator-defined region of interest (ROI). Each ROI was drawn by outlining the tumor border at each parametric map of the section including the longest diameter of the tumor. Percentage changes in diffusion- weighted MR and DCE-MR parameters relative to baseline were calculated as follows:

$\mathbf{Value\ Change}\ (\%) = (\mathbf{Value_{given\ time}} - \mathbf{Value_{baseline}})/\mathbf{Value_{baseline}} \times \mathbf{100.}$

Serum TNF-α Level Measurement

To ascertain whether CKD-516 up-regulated production of TNF-α, serum samples were collected from the central artery of the rabbit ear immediately prior to MR scanning at baseline, 4 hours, 24 hours, and 7 days. Using the enzyme-linked immunosorbent assay (ELISA) kit (Biorbyt, Cambridge, UK), TNF-α levels were measured in 9 rabbits (3 in G1, 3 in G3, and 3 in G4) according to the manufacturer's protocol.

Histologic Analysis

After MRI, all rabbits were sacrificed through intravenous injection of 5 mL of KCl under deep anesthesia and frozen at -70˚C in a plastic frame to maintain their posture in order to avoid misregistration between the pathologic MR images and pathologic specimen. Pathologic specimens were sectioned in the transverse plane with a 1 mm interval to match the MR images. For each tumor, a representative microscopic section which would be matched to the corresponding MR image was selected. For each tumor tissue, Hematoxylin and Eosin (H&E), terminal deoxynucleotidyl transferase mediated dUTP-biotin nick end labeling (TUNEL) staining

(Millipore, Bedford, MA, USA), and CD31 (Dako, Carpinteria, CA, USA) were performed to evaluate the necrotic fraction (NF), apoptosis, and blood vessel density of the tumor, respectively. Necrotic fraction can be calculated from the formula: $\mathbf{NF}\ (\%) = \mathbf{Area_{necrosis}}/\mathbf{Area_{total\ tumor}} \times \mathbf{100}$, in which can be measured by using the analysis software, ImageJ (http://rsb.info.nih.gov/ij). The apoptotic index (AI) was calculated as the average of the percentages of TUNEL-positive brown stained apoptotic cells from 3 randomly selected high-power fields (x400) of the tissue section avoiding the areas of necrosis (23). Among the 21 cases, 3 (one in G1, one in G2, and the other one in G3) were excluded in the analysis of AI due to poor staining quality. To obtain the histologic vascular parameter of the tumor, hot spots meaning higher vascular density areas compared to the rest of the tissue, were chosen at low magnification (x 40), and CD31 stained vessels were counted at high magnification (x 200, 0.544 mm^2). The mean of three measurements in the hot spots was used as the mean vessel density (MVD) of the tumor.

Statistical Analysis

To evaluate the reproducibility of IVIM-DWI and DCE-MR parameters,

measured values on baseline and 4 hour follow-up in the control group (n=6) were compared and corresponding coefficients of variation (CVs) within subjects were calculated. CVs of ≤10%, 10-25%, and ≥25% were considered to be of good, moderate, and poor reproducibility, respectively (24). Interobserver variability for size measurement on T2-weighted image was assessed using an intraclass correlation coefficient (ICC). ICC values ranged between -1 (perfect discordance) and +1 (perfect concordance). In order to determine whether there were differences in interval changes in tumor size, diffusion-weighted MR values, serum TNF-α levels, and histologic features between the control and treated group or among the treated groups of different dosage regimens, the Mann-Whitney test or Kruskal-Wallis test with post hoc comparison, were used.

For the animals that survived until the 7 day follow-up in the treated group, serial change in IVIM-DWI and DCE-MR parameters (n=15), and serum TNF-α levels (n=6) at different time points were evaluated using the Friedman test. In cases of statistical significance, further comparisons were performed using the post hoc Wilcoxon signed rank test. To determine whether IVIM-DWI and DCE-MR parameters can be early predictive indicators for tumor response, the Spearman rank correlation test was

performed to assess the correlation between the change in MR parameters at each time point compared to the baseline and the size change in tumor size at 7 day follow-up. In addition, Spearman rank correlation test was also performed to assess the correlation between MR parameters at 7 day follow-up and corresponding histologic features such as NF, AI, and MVD. To evaluate the correlation between the perfusion-related IVIM-DWI parameters (D^*, f, and fD^*) and DCE-MR parameters (K^{trans} and iAUC), Spearman rank correlation test was performed for measured MR values at baseline and 7 day follow-up in all subjects (n=21), and also for calculated relative percentage changes of follow-up MR parameters in the treated group (n=15). A P value of less than 0.05 was regarded to be of statistical significance except in the case of the post hoc Wilcoxon signed rank test (10 paired comparisons in 5 time points or 6 paired comparisons in 4 time points) in which a Bonferroni corrected P value of less than 0.005 (=0.05/10) or 0.008 (=0.05/6) was considered to indicate a statistical significance. All statistical analyses were performed using MedCalc software version 12.2.1.0 (MedCalc Software, Mariakerke, Belgium).

Figure 1. Baseline MR images including T2-weighted images and DWI in a rabbit VX2 liver tumor model. **(a)** T2-weighted image shows a 7 mm VX2 carcinoma in the liver left lobe. **(b)** DWI demonstrates a liver tumor with high signal intensity (*b* value=200 sec/mm^2). **(c)** ADC map and IVIM-DWI derived parametric maps of **(d)** *D*, **(e)** *D**, and **(f)** *f* were able to be obtained using prototype software on a pixel-by-pixel basis.

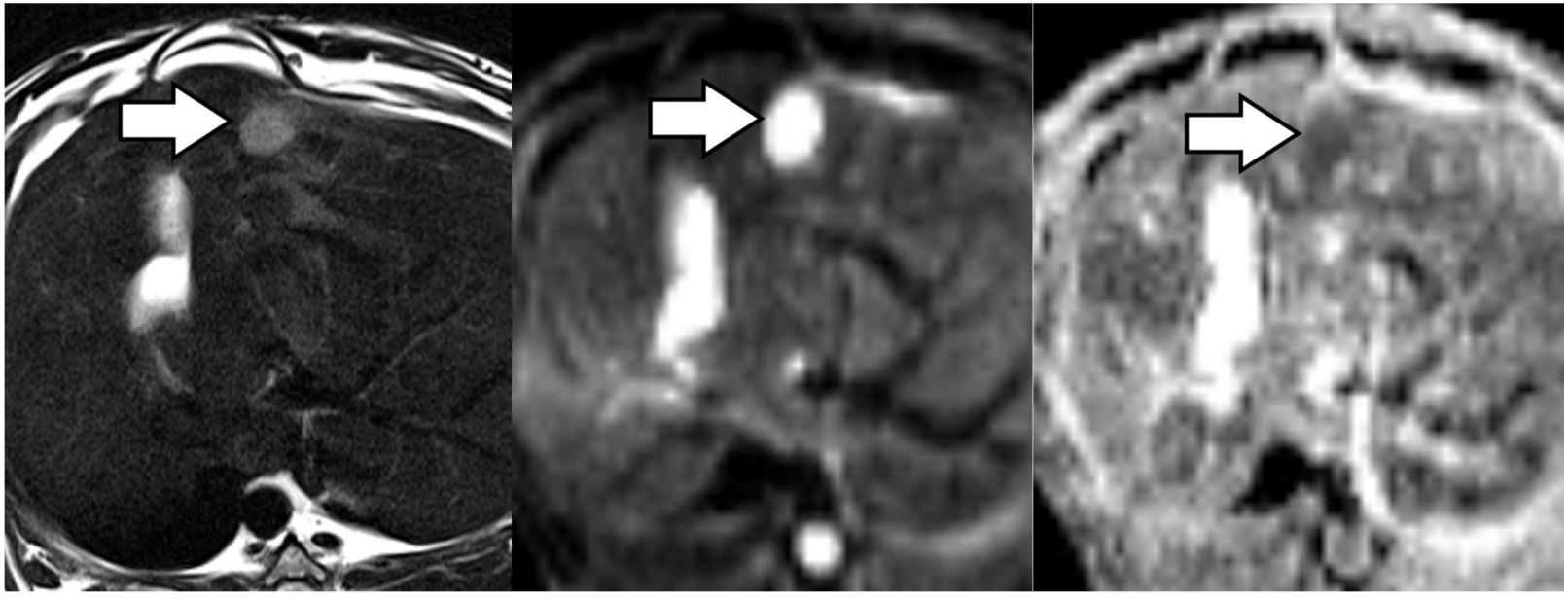

(a) **(b)** **(c)**

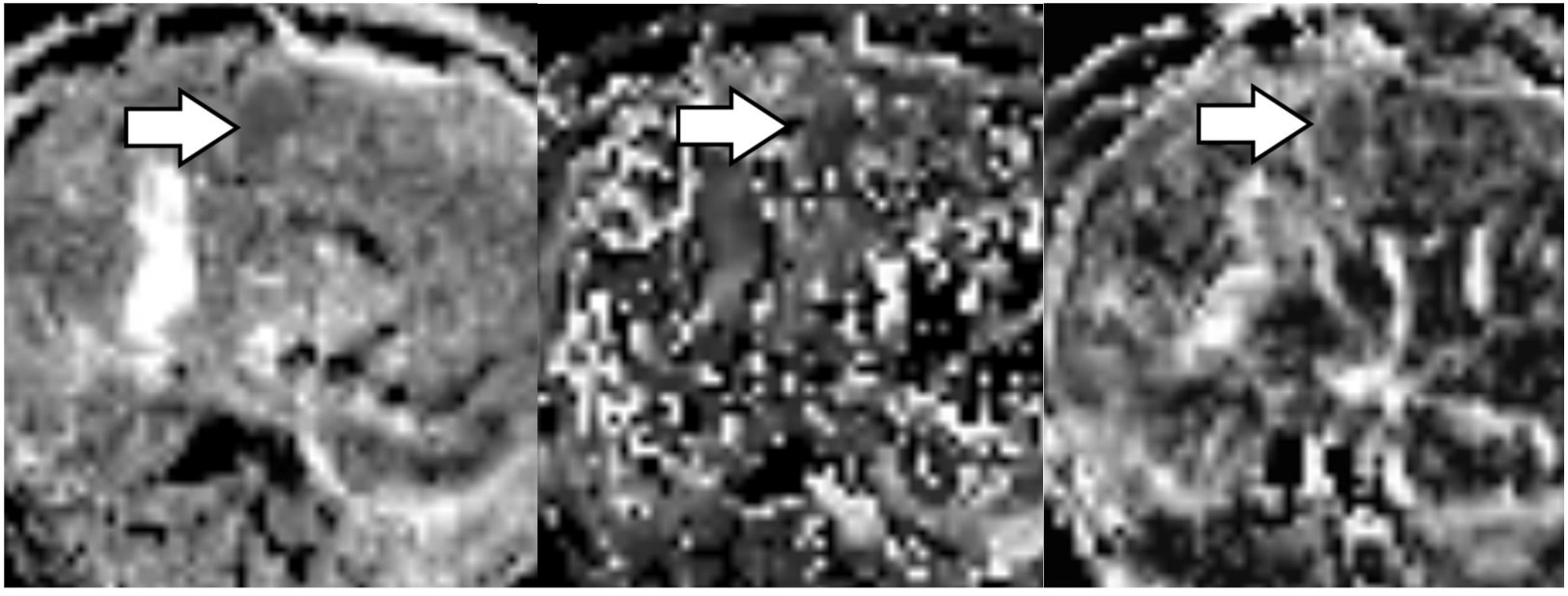

(d) **(e)** **(f)**

Figure 2. Creation of a perfusion map using prototype software. Using the DCE-MR images, voxel-wise perfusion maps can be obtained and quantitative perfusion-related values including K^{trans} and iAUC are automatically calculated by drawing an ROI outlining the entire tumor boundary.

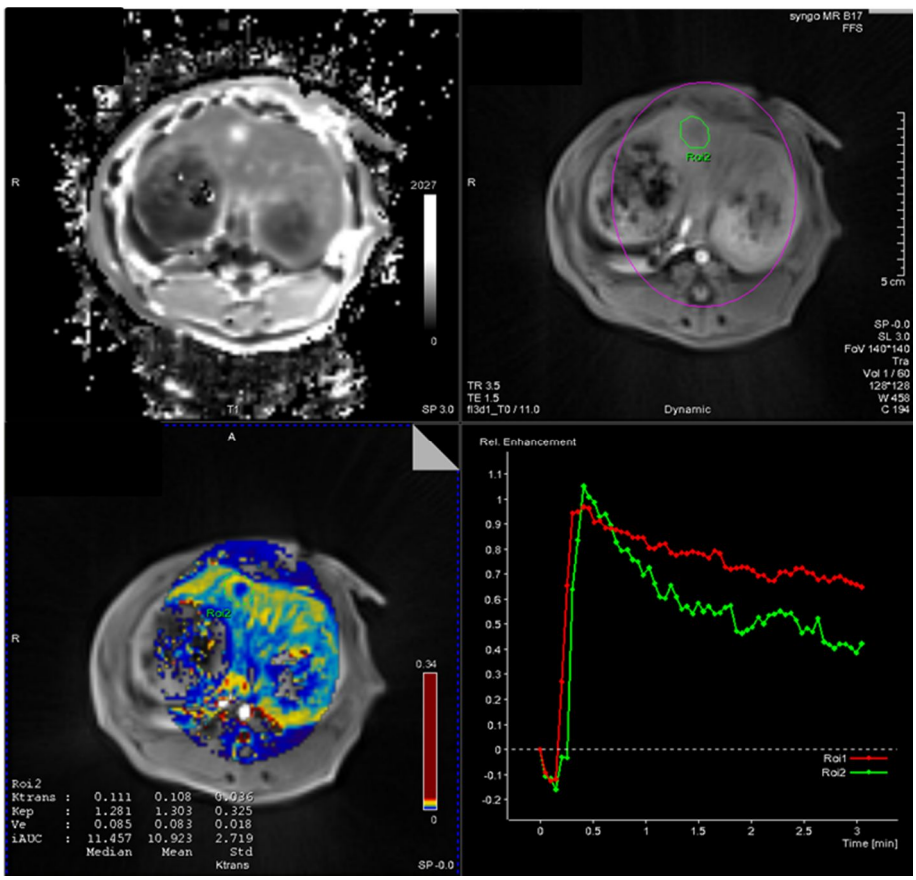

RESULTS

Effect of CKD-516 Treatment on Tumor Growth

At 7 day follow-up, the relative percentage change in tumor size of the tumors was significantly larger in the control group (median of 104.6%) than in the treated group (median of 65.6%) (P=0.005). Percentage increase in tumor size tended to be smaller in the treated group using a higher dosage of CKD-516 (medians of 70.9%, 65.6%, and 52.4% in G2, G3, and G4, respectively), however, there was no statistically significant difference among G2, G3, and G4 (P=0.40) (Table 1).

Inter-Observer Variability of Size Measurement

In the longest diameter measurement on T2-weighted images, inter-observer variability was good with an ICC of 0.90 (95% confidence interval, 0.77-0.96).

Serum TNF-α Levels: Serial Change after CKD-516 Treatment

The median values of the percentage changes of serum TNF-α relative to baseline for control (n=3) and treated group (n=6) at each time point are

summarized in Table 2. In the treated group, TNF-α significantly increased at 4 hour follow-up with a median of 3718.5% and decreased at 24 hours to almost baseline levels (median of 27.4%). The relative change was significantly different only at 4 hour follow-up between the control and treated groups (P=0.02). There was no statistically significant difference for all measurements between the subgroups of different dosage regimens (G3 and G4) (P>0.05). In the serial measurement of serum TNF-α in the treated group (n=6), median values of serum TNF-α were 5.8, 232.8, 18.1, and 11.8 pg/mL at baseline, 4 hour, 24 hour, and 7 days, respectively (Table 3) (Fig. 3). At 4 hour follow-up, CKD-516 up-regulated production of TNF-α (about 40-fold increase), however, the Friedman test followed by Wilcoxon signed rank test revealed no statistical significant difference among the different time points with P values of 0.03 (>0.008) each in the Wilcoxon test for 4 hour follow-up vs. baseline, 24 hour, and 7 day follow-up.

Histologic Features in Control and Treated Group

Histologic features including NF, AI, and MVD at 7 day follow-up demonstrated no statistically significant differences between the control and treated groups (P>0.05) and among the treated subgroups of different

dosage regimens (P>0.05).

Table 1. Comparison of Changes in Tumor Size Between Groups with Different Dosage Regimens of CKD-516

	G1 (n=6)	Treated (n=15)			P value*
		G2 (n=5)	G3 (n=5)	G4 (n=5)	
Δ Tumor Size (%)	104.6 (88.0; 141.6)		65.6 (27.5; 113.3)		0.005†
		70.9 (40.7; 113.3)	65.6 (50.5; 107.6)	52.4 (27.5; 81.1)	0.40

Note. – Data are medians. Data in parentheses are ranges. Relative change (Δ) of tumor size was determined by comparing the longest diameter at baseline and that at 7 day follow-up. *Data were tested with the Mann-Whitney test (G1 vs. Treated group) or Kruskal-Wallis test (G2 vs. G3 vs. G4). †Significant value, P<0.05. G1=control group; G2, G3, and G4= treated group with 5, 9, and 12 mg/m^2 of CKD-516.

Table 2. Comparison of Changes in Serum TNF-α Level in the Control (n=3) and Treated Groups (n=6)

Δ TNF-α (%)	Control (n=3)	Treated (n=6)	P value*
4 hours	-27.2 (-47.4; 3.7)	3718.5 (291.9; 21926.7)	0.02†
24 hours	-13.5 (-51.3; 42.4)	27.4 (-94.7; 1590.5)	0.61
7 days	6.1 (-35.0; 194.7)	91.2 (-58.5; 772.4)	0.80

Note. – Data are medians. Data in parentheses are ranges. Relative change (Δ) was determined by comparing the value of baseline and that of follow-up. *All data were tested with the Mann-Whitney test. †Significant value, P<0.05.

Table 3. Serial Measurements of Serum TNF-α Level in the Treated Group and P Values of Comparisons Between Different Time Points

TNF-α (pg/mL)	Measurement	P value*		
		4 hours	24 hours	7 days
Pre	5.8 (1.9; 22.9)	0.03	n.s.	n.s.
4 hours	232.8 (18.0; 419.0)		0.03	n.s.
24 hours	18.1 (0.2; 42.5)			0.03
7 days	11.8 (3.5; 22.4)			

Note. – Data are medians. Data in parentheses are ranges. *All data were tested with Friedman test followed by Wilcoxon signed rank test in cases of statistical significance. n.s.=not significant in the Friedman test. †Significant value, P<0.008.

Part 1. IVIM-DWI

Inter-Study Reproducibility of ADC and IVIM Parameters

In six rabbits of the control group, ADC and *D* demonstrated good reproducibility with CVs within subjects of 6.7% and 3.0%, respectively. D^*, and *f* showed moderate reproducibility with CVs of 11.9% and 13.7%, respectively.

Comparison of ADC and IVIM Parameters Between the Control and Treated Group

The median values of the percentage change of ADC and three IVIM parameters relative to baseline for each group at each time point are summarized in Table 4.

Percentage change of ADC was significantly higher in the treated group than in the control at 24 hour follow-up (medians of +14.2% vs. -4.4%, P=0.02). For *D,* although the relative change of *D* at 24 hour follow-up was higher in the treated group than in the control group (medians of +11.2% vs. +0.2%), there was no significant difference between the treated group and control from baseline (P=0.12). D^* in the treated group significantly decreased compared to the control group at 4 hour follow-up (medians of -

37.3% vs. +0.2%, P<0.001) and there was no significant difference between the treated group and the control group at 24 hour follow-up. Relative changes in *f* values were significantly lower in the treated group than the control at both 4 hour and 24 hour follow-ups (medians of -51.1% vs. -7.6%, P=0.001 and -24.1% vs. -1.5%, P=0.02). At 4 hour follow-up, relative change in fD^* in the treated group was significantly lower than in the control group (medians of -69.9% vs. -5.7%, P<0.001).

All the relative changes of ADC and IVIM parameters showed no significant differences between the control and treated groups at 3 day and 7 day follow-ups. For all relative changes of parameters at any follow-up time points, there were no statistically significant differences among the treated subgroups of different dosage regimens (G2, G3, and G4).

Serial Measurements of ADC and IVIM Parameters in the Treated Group

Results of the Friedman test followed by Wilcoxon signed rank test for serial measurements of ADC and three IVIM parameters are summarized in Table 5.

Serial measurements of ADC and *D* in the treated group demonstrated

that ADC and *D* slightly decreased at 4 hour follow-up, although it was not statistically significant, and significantly increased at 24 hours compared to that at baseline (in *D*, P=0.003), and/or 4 hour follow-up (in ADC and *D*, P=0.003 and <0.001, respectively). At 3 day and 7 day follow-ups, those values gradually decreased compared to those at 24 hours although it did not show a statistically significant difference (Figs. 4a and 4b).

D^* significantly decreased at 4 hour follow-up from a median of 40.4 to 25.8 (x 10^{-3} mm^2/sec) (P<0.001), but it recovered at 24 hour follow-up with a median of 35.2 (x 10^{-3} mm^2/sec) which demonstrated no significant difference compared to that at baseline. There was no statistically significant difference among the D^* values at 24 hours, 3 days, and 7 days (Fig. 4c).

f markedly decreased at 4 hour follow-up from a median of 17.7% to 9.8% (P<0.001), partially recovered at 24 hour follow-up with a median of 13.5% but was lower than that of baseline (P=0.007). At 3 day follow-up, *f* recovered to the median of 18.8% which showed no statistically significant difference between baseline and 3 day follow-up (P>0.05). However, *f* decreased at 7 day follow-up with a median of 12.1% compared to that at baseline and that at 3 days (P=0.002 and <0.001, respectively) (Fig. 4d).

fD^* significantly decreased at 4 hour follow-up (P<0.001) and partially recovered at 24 hour and 3 day follow-up, which showed no statistical significant differences compared to baseline (P>0.005) (Fig. 4e).

Early Prediction of Tumor Response with Changes in ADC and IVIM Parameters

To evaluate the feasibility of ADC and IVIM parameters for prediction of tumor response, correlation between the percentage increases in tumor size and change in the ADC and IVIM parameters were assessed (Table 6). Among the parameters, relative changes in *f* and fD^* values at 4 hour follow-up showed a statistically significant correlation with tumor response with a Spearman rho of 0.53 and 0.65 with P values of 0.04 and 0.009, respectively, which meant that a greater decrease in *f* and fD^* at 4 hours would predict a smaller increase in tumor size at 7 days (Fig. 5). Relative change in *f* and fD^* at 7 day follow-up showed significant correlation with changes in tumor size (Spearman rho of -0.66 and -0.55; P=0.008 and 0.04, respectively), which reflected the fact that increases in tumor size would result in decreases in *f* and fD^*.

Correlation of Histologic Features with ADC and IVIM Parameters

In the 21 rabbits (6 in the control group and 15 in the treated group) which survived during the entire experimental period, DWI parameters including ADC and three IVIM parameters at 7 day follow-up images and corresponding histologic features including NF, AI, and MVD were correlated (Table 7). NF was significantly correlated with ADC and *D* (rho=0.59 and 0.68; P=0.005 and <0.001, respectively) (Fig. 6). MVD showed significant correlation with perfusion-related parameters *f* and fD^* (rho=0.52 and 0.62; P=0.02 and 0.003) (Fig. 7). However, D^* did not show a statistically significant correlation with MVD (rho=0.27, P=0.24). In addition, AI showed no significant correlation with any of the IVIM-DWI parameters (P>0.05).

Part 2. DCE-MRI

Inter-Study Reproducibility of DCE-MR Parameters

In six rabbits of the control group, K^{trans} and iAUC showed good reproducibility with CVs within subjects of 9.6% and 7.5%, respectively.

Comparison of DCE-MR Parameters Between the Control and Treated Group

Among DCE-MRI studies, one case in G1 at 3 day follow-up and one case in G4 at 24 hours were excluded from quantitative analysis due to inappropriate MR data caused by extensive respiratory motion. The median values of the percentage change of DCE-MR parameters relative to baseline for each group at each time point are summarized in Table 4. DCE-MR parameters (both K^{trans} and iAUC) significantly decreased in the treated group compared to those of control at 4 hour and 24 hour follow ups (medians of -4.1% vs. -25.8% at 4 hours, -13.8% vs. -24.5% at 24 hours for K^{trans}; and -4.6% vs. -36.6% at 4 hours, -9.6% vs. -26.4% at 24 hours for iAUC) ($P<0.05$). All relative changes of DCE-MR parameters showed no significant differences between the control and treated groups at 3 day and 7 day follow-ups ($P>0.05$). For all relative changes of parameters at any

follow-up time points, there were no statistically significant differences among the treated subgroups of different dosage regimens (G2, G3, and G4).

Serial Measurements of DCE-MR Parameters in the Treated Group

To evaluate serial change in DCE-MR parameters in the CKD-516 treated group (n=14), the Friedman test followed by Wilcoxon signed rank test was performed and the results are summarized in Table 5. Both K^{trans} and iAUC significantly decreased at 4 hour follow-up compared to those at baseline ($P<0.005$) (Fig. 8), and they were persistently low at 24 hour follow-up although P values from the post hoc Wilcoxon test were 0.007 and 0.008 (>0.005) compared to baseline values, respectively. At 3 day follow-up, K^{trans} and iAUC almost recovered to baseline ($P>0.05$ on the Friedman test) (Figs. 4f and 4g). K^{trans} and iAUC significantly decreased at 7 day follow-up compared to those at 3 day follow-up ($P=0.002$ and 0.003, respectively), however, it was also observed in the control group as described above.

Early Prediction of Tumor Response with Change in DCE-MR Parameters

To evaluate the feasibility of DCE-MR parameters including K^{trans} and iAUC for prediction of tumor response, correlation between the percentage increases in tumor size and changes in DCE-MR parameters were assessed (Table 6). As a result, none of the relative changes in DCE-MR parameters at each time point showed significant correlation with change in tumor size ($P>0.05$).

Correlation of Histologic Features with DCE-MR Parameters

In the 21 rabbits (6 in the control group and 15 in the treated group), DCE-MR parameters at 7 day follow-up image and corresponding histologic features including NF, AI, and MVD were correlated. However, none of NF, AI, and MVD revealed significant correlation with DCE-MR parameters ($P>0.05$) (Table 7).

Table 4. Relative Changes in IVIM-DWI and DCE-MR Parameters at Follow-up Studies in the Control and Treated Groups

IVIM-DWI parameters	Control (n=6)	Treated (n=15)	P value*
Δ ADC (%)			
4 hours	3.0 (-10.0; 16.4)	-9.6 (-28.1; 22.3)	0.21
24 hours	-4.4 (-10.3; 5.9)	14.2 (-20.1; 47.0)	0.02†
3 days	2.7 (-16.9; 11.4)	12.4 (-27.8; 58.9)	0.12
7 days	-0.7 (-21.9; 14.2)	-8.3 (-34.1; 60.2)	0.70
Δ *D* (%)			
4 hours	-1.5 (-7.1; 0)	-8.9 (-35.6; 26.9)	0.35
24 hours	0.2 (-9.1; 18.9)	11.2 (-20.2; 47.6)	0.12
3 days	-8.4 (-18.7; 25.5)	7.0 (-17.7; 52.2)	0.10
7 days	-11.2 (-25.1; 33.8)	-5.0 (-30.0; 55.6)	0.64
Δ D^* (%)			
4 hours	0.2 (-13.9; 44.4)	-37.3 (-59.7; 23.9)	<0.001†
24 hours	3.0 (-31.1; 32.2)	-13.4 (-50.2; 38.0)	0.48
3 days	-0.2 (-29.1; 60.5)	-24.5 (-54.7; 97.6)	0.24
7 days	4.7 (-36.6; 31.1)	-15.7 (-62.7; 42.1)	0.31
Δ *f* (%)			
4 hours	-7.6 (-23.3; 25.0)	-51.1 (-72.8; -7.7)	0.001†
24 hours	-1.5 (-17.8; 32.9)	-24.1 (-62.2; 58.4)	0.02†

3 days	2.4 (-45.4; 80.7)	4.4 (-58.9; 56.3)	1.00
7 days	-12.3 (-71.9; 50.7)	-38.0 (-74.0; 41.4)	0.31
Δ *fD** (%)			
4 hours	-5.7 (-34.0; 80.5)	-69.9 (-85.1; -57.1)	<0.001†
24 hours	-2.8 (-38.5; 75.7)	-33.6 (-68.3; 105.2)	0.05
3 days	-9.4 (-49.3; 141.5)	-22.8 (-69.7; 201.2)	0.48
7 days	-14.4 (-82.2; 57.8)	-47.8 (-85.9; 100.9)	0.24
DCE-MR parameters	Control (n=5, 6)‡	Treated (n=14, 15)‡	P value*
Δ K^{trans} (%)			
4 hours	-4.2 (-17.4; 25.6)	-25.8 (-72.8; 27.6)	0.01†
24 hours	-13.8 (-18.5; 1.2)	-24.5 (-69.1; 38.8)	0.03†
3 days	30.5 (-13.3; 51.3)	2.4 (-27.0; 45.8)	0.24
7 days	-8.0 (-46.0; 63.8)	-37.3 (-73.5; 22.8)	0.16
Δ iAUC (%)			
4 hours	-4.6 (-20.3; 5.0)	-36.6 (-86.5; 24.2)	0.01†
24 hours	-9.6 (-14.3; -2.1)	-9.6 (-14.3; -2.1)	0.02†
3 days	-2.4 (-27.0; 45.8)	-20.5 (-60.0; 66.1)	0.51
7 days	-18.0 (-45.0; 71.7)	-39.5 (-87.9; 25.8)	0.21

Note. – Data are medians. Data in parentheses are ranges. Relative change (Δ) was determined by comparing the value of baseline and that of follow-up. *All data were tested with the Mann-Whitney test. †Significant value, P<0.05. ‡Number of subjects

were 6 in the control group except 3 day follow-up (n=5) and 15 in the treated group except 24 hour follow-up (n=14).

Table 5. Serial Measurements of IVIM-DWI and DCE-MR Parameters in the Treated Group and P Values of Comparisons Between Different Time Points

Parameter	Measurement	P value*			
		4 hours	24 hours	3 days	7 days
IVIM-DWI (n=15)					
ADC (x 10^{-3} mm^2/sec)					
Pre	1.00 (0.80; 1.17)	n.s.	n.s.	n.s.	n.s.
4 hours	0.94 (0.78; 1.09)		0.003†	0.007	n.s.
24 hours	1.13 (0.80; 1.32)			n.s.	0.008
3 days	1.11 (0.76; 1.62)				0.01
7 days	0.96 (0.66; 1.44)				
D (x 10^{-3} mm^2/sec)					
Pre	0.92 (0.76; 1.07)	n.s.	0.003†	n.s.	n.s.
4 hours	0.84 (0.63; 1.05)		<0.001†	0.02	n.s.
24 hours	1.06 (0.74; 1.32)			n.s.	0.02
3 days	1.03 (0.75; 1.52)				n.s.
7 days	0.89 (0.65; 1.39)				
D^* (x 10^{-3} mm^2/sec)					
Pre	40.4 (24.0; 66.9)	<0.001†	n.s.	n.s.	0.06
4 hours	25.8 (13.4; 33.7)		<0.001†	0.007	0.008

24 hours	35.2 (19.6; 61.4)			n.s.	n.s.
3 days	32.5 (23.0; 48.5)				n.s.
7 days	34.1 (21.7; 52.8)				
f (%)					
Pre	17.7 (13.7; 27.0)	<0.001†	0.007	n.s.	0.002†
4 hours	9.8 (4.4; 17.9)		0.003†	<0.001†	n.s.
24 hours	13.5 (6.1; 21.7)			0.17	0.12
3 days	18.8 (10.6; 24.7)				<0.001†
7 days	12.1 (6.0; 22.2)				
fD^* (x 10^{-3} mm^2/sec)					
Pre	8.2 (3.8; 10.6)	<0.001†	0.01	n.s.	0.001†
4 hours	2.9 (0.6; 3.9)		<0.001†	<0.001†	n.s.
24 hours	4.5 (1.2; 13.3)			n.s.	0.08
3 days	5.9 (3.1; 12.0)				0.01
7 days	3.8 (1.3; 7.6)				
DCE-MRI (n=14)					
K^{trans} (min^{-1})					
Pre	0.13 (0.09; 0.19)	0.002†	0.007	n.s.	0.005
4 hours	0.09 (0.04; 0.13)		n.s.	0.04	n.s.
24 hours	0.09 (0.04; 0.19)			0.04	n.s.
3 days	0.13 (0.06; 0.25)				0.002†

7 days	0.09 (0.04; 0.15)				
iAUC (mmol/sec)					
Pre	15.1 (10.5; 22.1)	<0.001†	0.009	n.s.	0.009
4 hours	10.5 (2.4; 13.5)		n.s.	0.02	n.s.
24 hours	10.3 (3.8; 21.4)			0.05	n.s.
3 days	13.7 (7.2; 28.9)				0.003†
7 days	11.0 (2.0; 17.7)				

Note. – Data are medians. Data in parentheses are ranges. *All data were tested with Friedman test followed by Wilcoxon signed rank test in cases of statistical significance. n.s.=not significant in the Friedman test. †Significant value, P<0.005.

Table 6. Correlation Between Changes in Tumor Size and Serial Change in IVIM-DWI and DCE-MR Parameters in the Treated Group (n=15)

Parameter	Correlation Coefficient¥	P value*
IVIM-DWI (n=15)		
Δ ADC (%)		
4 hours	-0.19	0.51
24 hours	-0.29	0.30
3 days	-0.48	0.07
7 days	-0.13	0.66
Δ *D* (%)		
4 hours	0.17	0.55
24 hours	0.07	0.80
3 days	-0.07	0.80
7 days	0.06	0.83
Δ D^* (%)		
4 hours	-0.06	0.83
24 hours	-0.32	0.25
3 days	-0.23	0.41
7 days	-0.2	0.47
Δ *f* (%)		

4 hours	0.53	0.04†
24 hours	0.03	0.91
3 days	-0.43	0.11
7 days	-0.66	0.008†
Δ *fD** (%)		
4 hours	0.65	0.009†
24 hours	-0.05	0.86
3 days	-0.41	0.13
7 days	-0.55	0.04†
DCE-MRI (n=14, 15)‡		
Δ K^{trans} (%)		
4 hours	0.30	0.28
24 hours	0.34	0.24
3 days	0.25	0.36
7 days	0.11	0.69
Δ iAUC (%)		
4 hours	0.31	0.25
24 hours	0.31	0.27
3 days	0.16	0.56
7 days	0.11	0.70

Note. –Relative change (∆) was determined by comparing the value of baseline and that of follow-up. [*]All data were tested with Spearman rank correlation test. [†]Significant value, P<0.05. [‡]Number of subjects were 6 in the control group except 3 day follow-up (n=5) and 15 in the treated group except 24 hour follow-up (n=14). [¥]Spearman correlation coefficient (rho).

Table 7. Correlation Between Histologic Features and IVIM-DWI and DCE-MR Parameters at 7 Day Follow-up

Parameter	MVD (n=21)		NF (%) (n=21)		AI (%) (n=18)	
	Correlation Coefficient‡	P value*	Correlation Coefficient‡	P value*	Correlation Coefficient‡	P value*
IVIM-DWI						
ADC (x 10^{-3} mm^2/sec)	-0.06	0.80	0.59	0.005†	0.23	0.37
D (x 10^{-3} mm^2/sec)	-0.14	0.55	0.68	<0.001†	0.13	0.60
D^* (x 10^{-3} mm^2/sec)	0.27	0.24	-0.14	0.54	0.09	0.72
f (%)	0.52	0.02†	0.03	0.89	-0.34	0.17
fD^* (x 10^{-3} mm^2/sec)	0.62	0.003†	-0.09	0.71	-0.18	0.48
DCE-MRI						
K^{trans} (min^{-1})	-0.02	0.95	-0.21	0.35	-0.26	0.29
iAUC (mmol/sec)	0.05	0.84	-0.25	0.28	-0.21	0.41

Note. – *All data were tested with Spearman rank correlation test. †Significant value, P<0.05. ‡Spearman correlation coefficient (rho). MVD=mean vessel density. NF=necrotic fraction. AI=apoptotic index

Figure 3. Graphs showing serial measurements of serum TNF-α level in the control (dashed line) and treated groups (solid line). Lines connect medians at different time points and error bars demonstrated upper and lower quartiles.

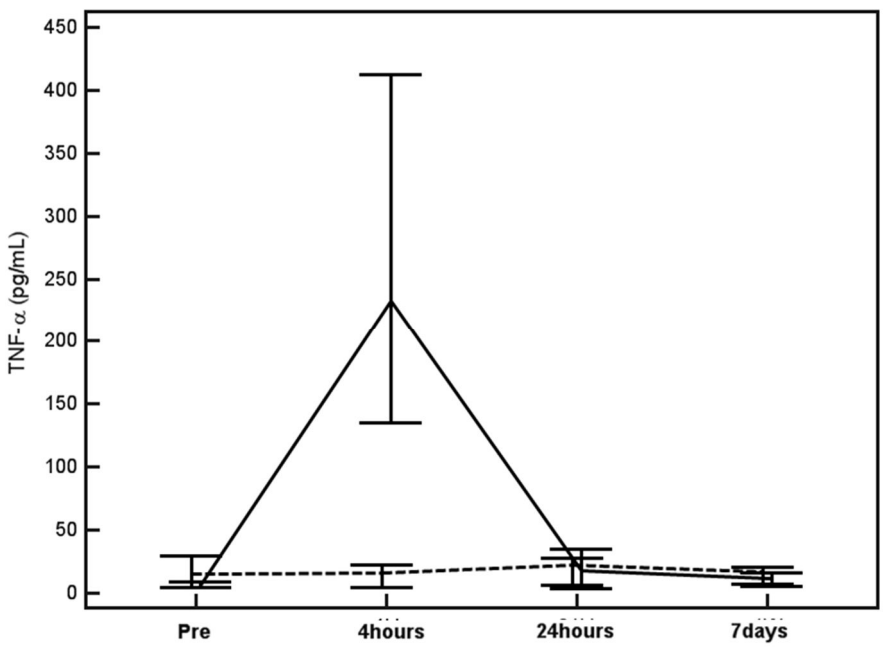

Figure 4. Graphs showing serial changes of **(a)** ADC and three IVIM parameters - **(b)** *D*, **(c)** D^*, **(d)** *f*, **(e)** fD^* -, as well as DCE-MR parameters - **(f)** K^{trans} and **(g)** iAUC - of the tumor in the control (dashed line) and treated groups (solid line) compared to baseline. Lines connect medians at different time points and error bars demonstrate upper and lower quartiles.

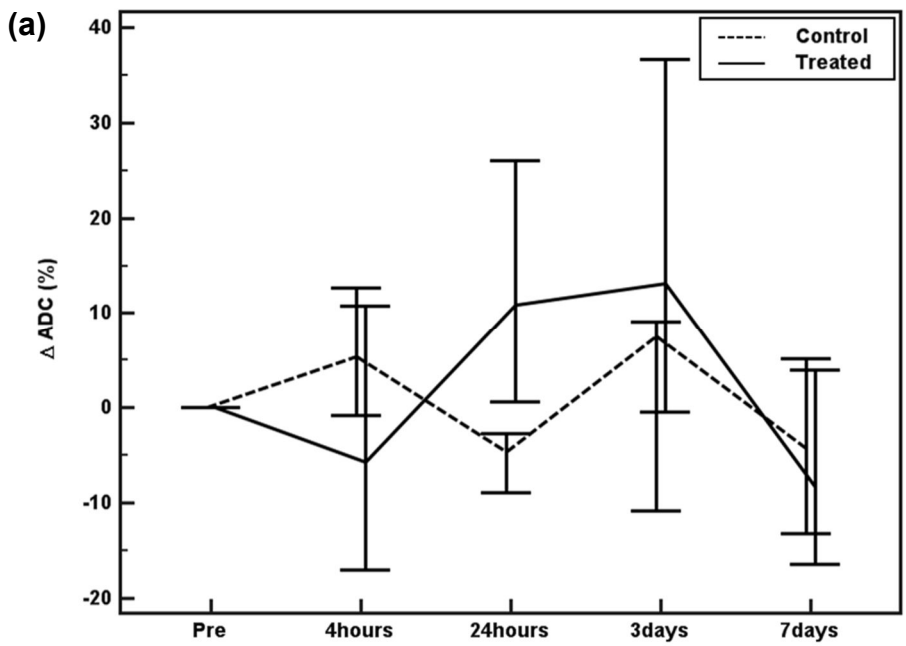

(b)

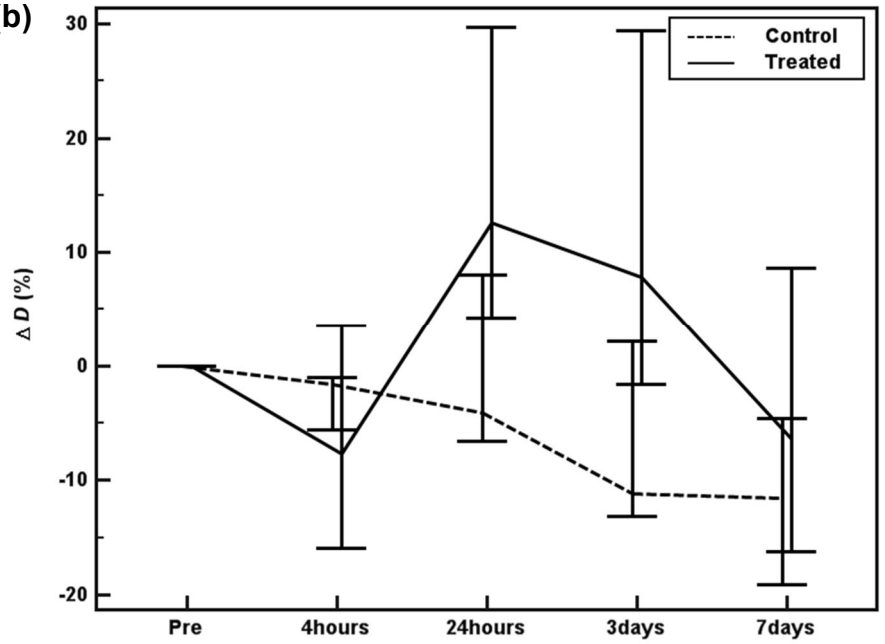
Control
Treated
Δ D (%)
30
20
10
0
-10
-20
Pre
4hours
24hours
3days
7days

(c)

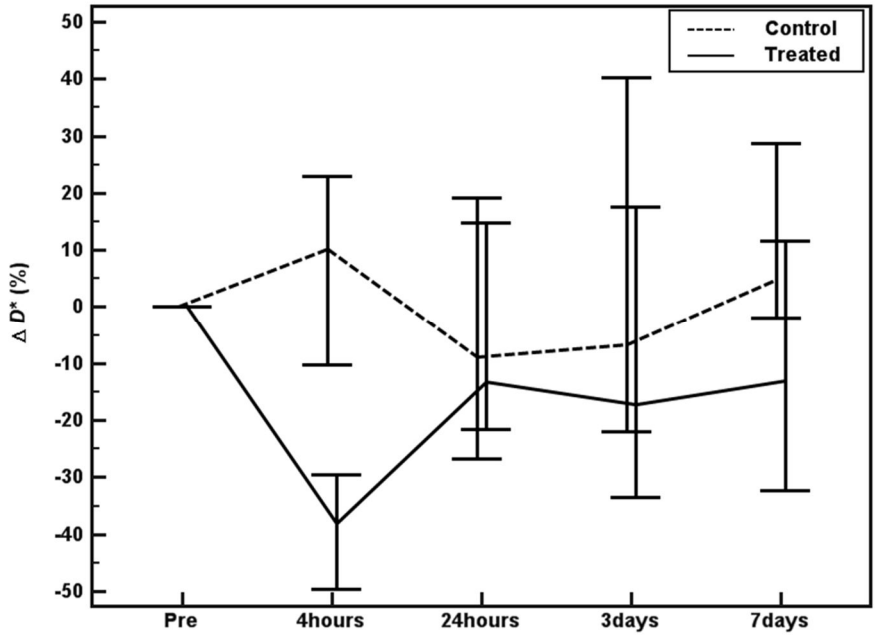
Control
Treated
Δ D* (%)
50
40
30
20
10
0
-10
-20
-30
-40
-50
Pre
4hours
24hours
3days
7days

(d)

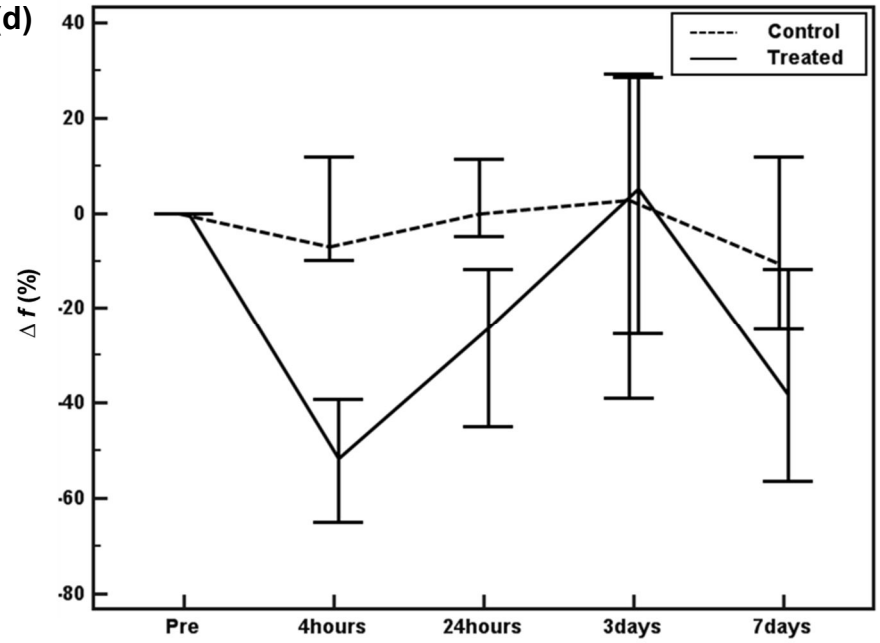
Control
Treated
40
20
0
-20
-40
-60
-80
Δ f (%)
Pre
4hours
24hours
3days
7days

(e)

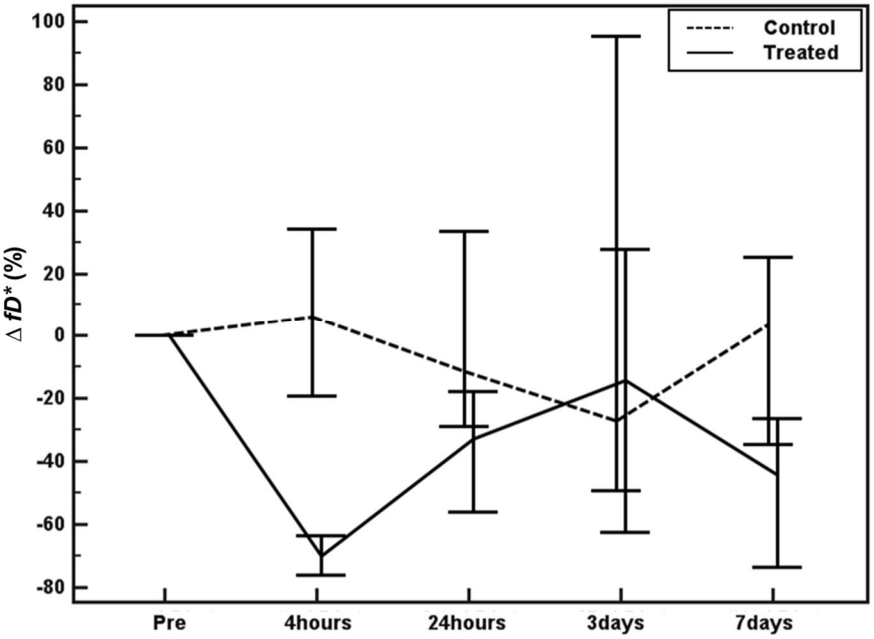
Control
Treated
100
80
60
40
20
0
-20
-40
-60
-80
Δ fD* (%)
Pre
4hours
24hours
3days
7days

(f)

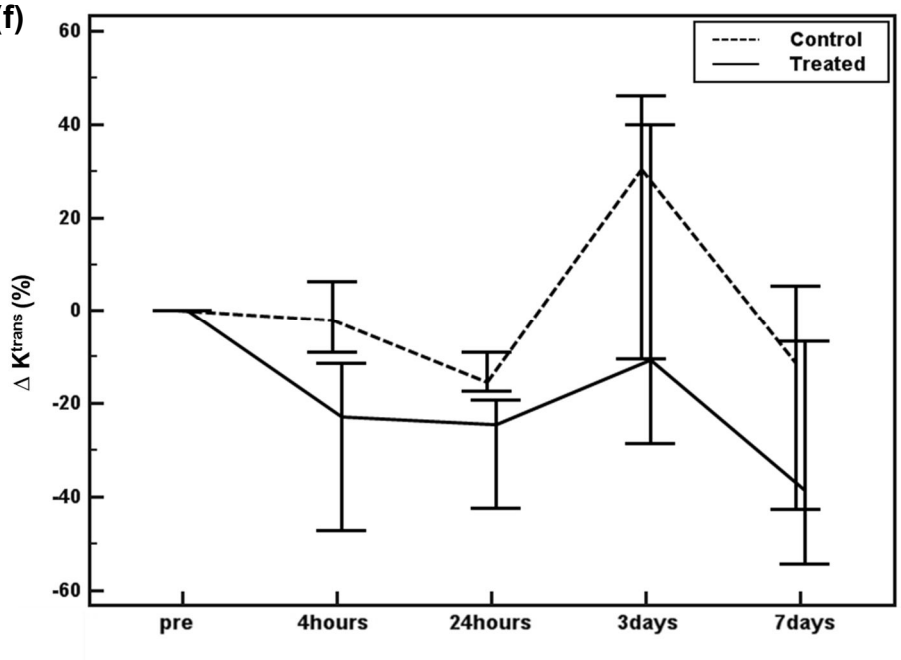
Control
Treated
60
40
20
0
-20
-40
-60
Δ K^trans (%)
pre
4hours
24hours
3days
7days

(g)

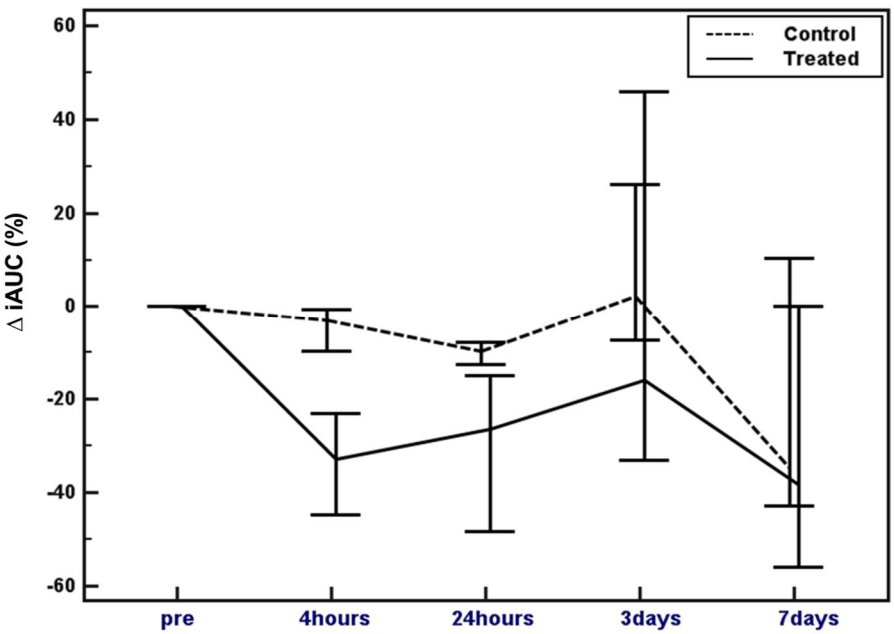
Control
Treated
60
40
20
0
-20
-40
-60
Δ iAUC (%)
pre
4hours
24hours
3days
7days

Figure 5. Graphs demonstrating the relationship between changes in tumor size during the experimental period of 7 days and relative change in **(a)** *f* and **(b)** fD^* at 4 hours compared to baseline. Significant correlations with rhos of **(a)** 0.53 (P=0.04) and **(b)** 0.65 (P=0.009) is observed.

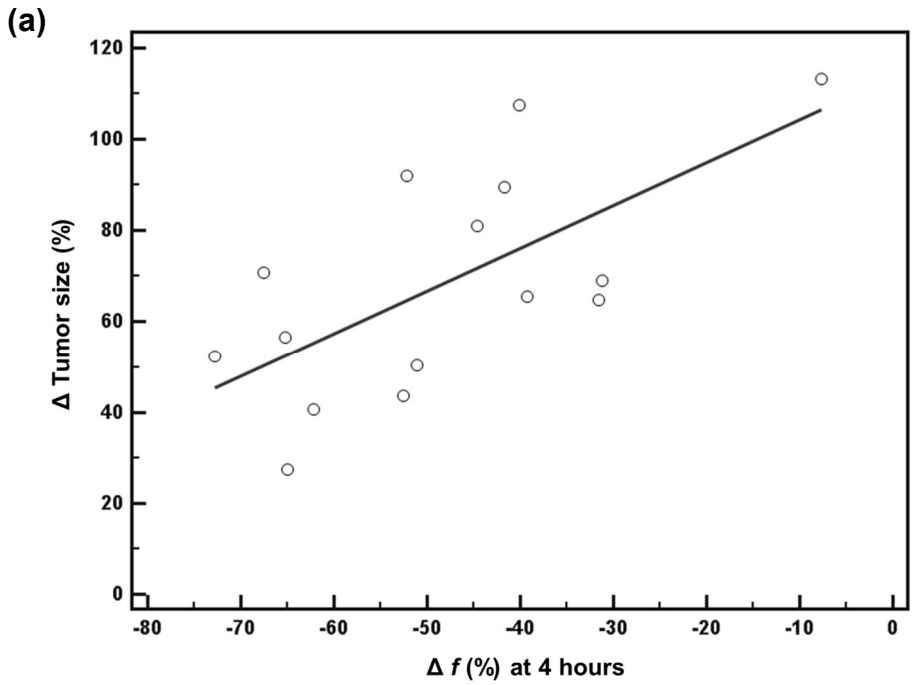

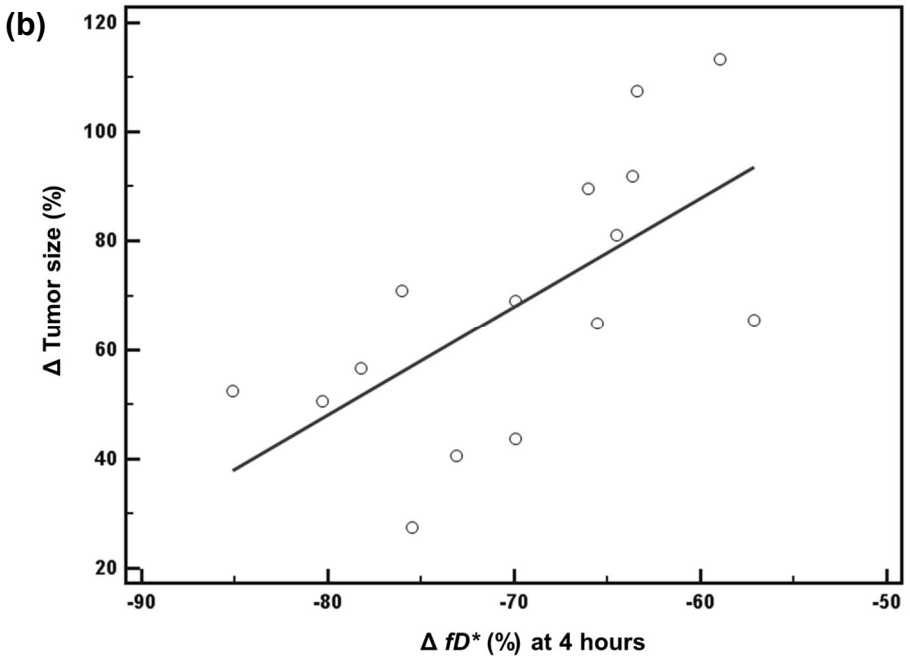
(b)
120
100
80
60
40
20
Δ Tumor size (%)
-90
-80
-70
-60
-50
Δ fD* (%) at 4 hours

Figure 6. *D* (true diffusion coefficient) and necrotic fraction of VX2 tumors (a and b: tumor with more necrosis, c and d: tumor with less necrosis) at 7 day follow-up. The measured *D* value of the tumor was 1.02 x 10^{-3} mm^2/sec **(a)** and corresponding histologic specimen (H&E stain) **(b)** shows large central necrosis and peripheral viable tumor tissue with a necrotic fraction of 26.1%. Another tumor with a measured *D* value of 0.89 x 10^{-3} mm^2/sec **(c)** shows a smaller necrotic fraction (16.5%) on the histologic specimen **(d)** (thick outer line: tumor border, thin inner line: necrotic portion).

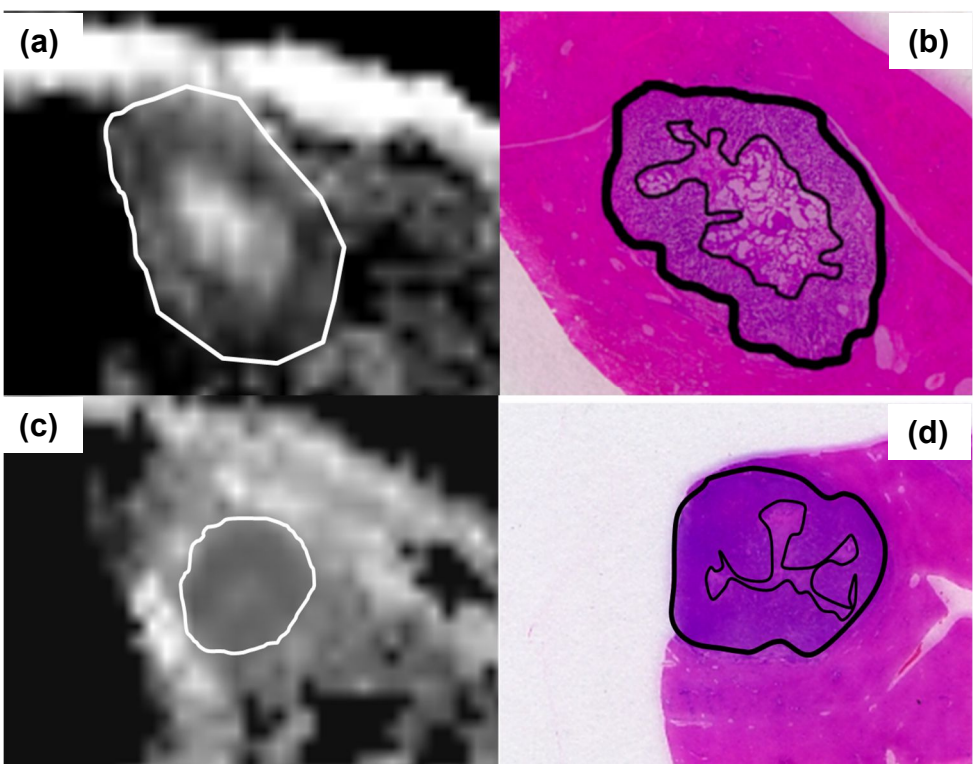

Figure 7. *f* (perfusion fraction) and microvessels (CD31 staining) of the VX2 tumors at 7 day follow-up. **(a and c)** *f* maps extracted from IVIM-DWI and **(b and d)** corresponding microscopic findings of tumors (x 200, CD31 staining), respectively. The tumor with higher *f* value (16.1%) **(c)** shows more prominent septa and abundant CD31-stained microvessels **(d)** than the tumor with lower *f* value (7.1%) **(a)** which has compact tumor cells and sparse microvessels **(b)**.

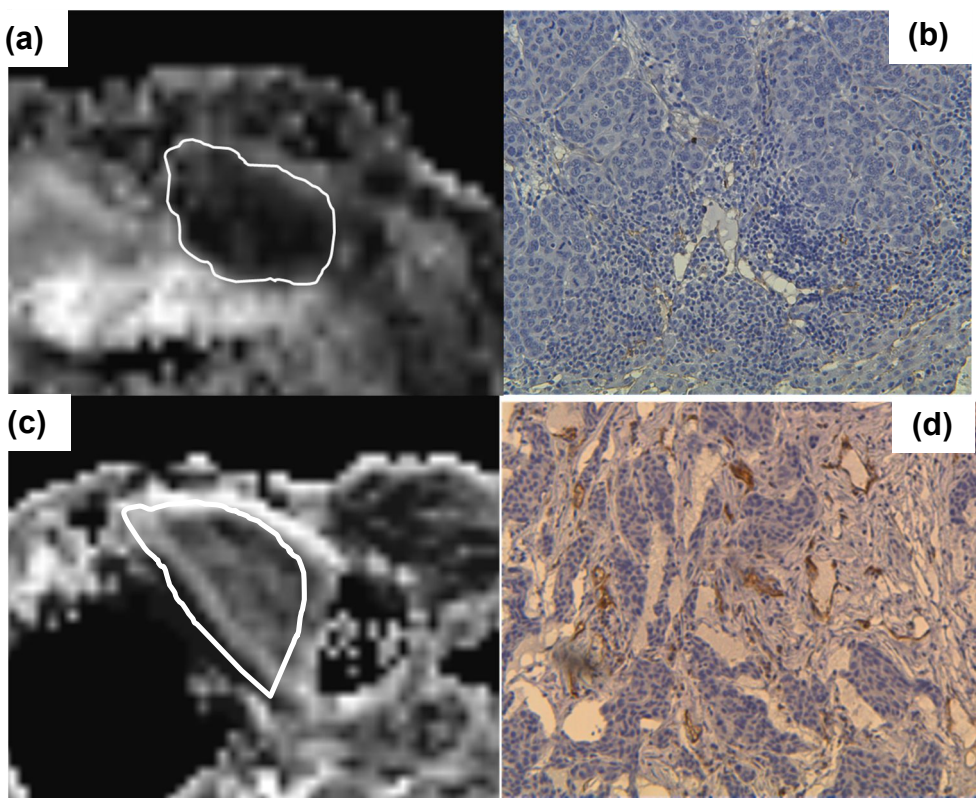

Figure 8. Changes of DCE-MR parameters after CKD-516 treatment. K^{trans} maps show a marked reduction of K^{trans} of the tumor: mean of 0.074 min^{-1} at baseline (a) to 0.038 min^{-1} at 4 hour follow-up (c). Time-intensity curve demonstrates a rapid increase of signal intensity within the tumor at the baseline study (b), however, at 4 hour follow-up, gradual increase of the signal intensity with lower peak intensity (red line: aorta, green line: tumor) resulting in lower iAUC value is shown.

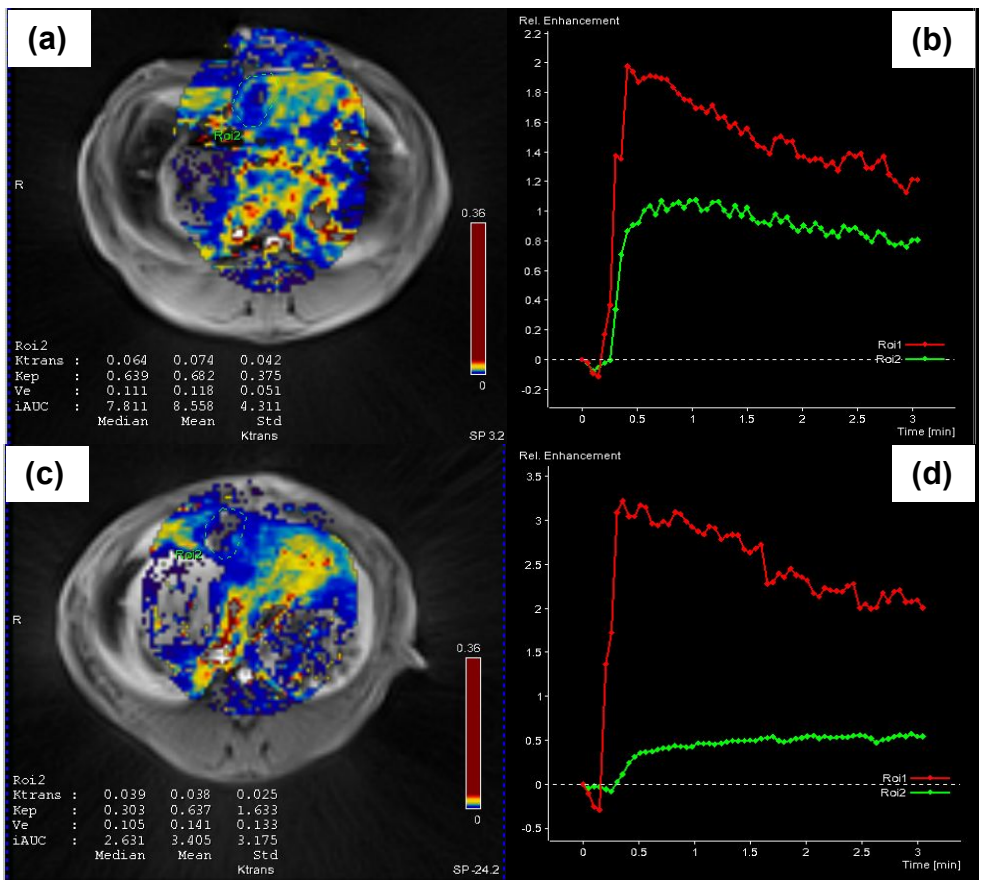

Part 3. Correlation Between IVIM-DWI and DCE-MRI

Correlation in Measured Values at Baseline and 7 Day Follow-up Between IVIM-DWI Parameters and DCE-MR Parameters

From the baseline and 7 day follow-up MR data of all subjects of the control and treated subjects (n=21), no significant correlation was found between each of the perfusion-related IVIM parameters (D^*, f, and fD^*) with DCE-MR parameters (K^{trans} and iAUC) (Table 8). However, although there was no statistical significance (P>0.05), positive trends were observed between IVIM-DWI parameters (f and fD^*) and DCE-MR parameters (K^{trans} and iAUC) with rhos from 0.31 to 0.37 at 7 day follow-up.

Correlation in Relative Change at Each Time Point Between IVIM-DWI Parameters and DCE-MR Parameters

At 4 hour follow-up, relative change in fD^* compared to baseline values showed a significant correlation with relative change in K^{trans} (rho=0.54, P=0.04) (Fig. 9). In addition, I observed positive trends between relative changes in fD^* and iAUC, D^* and iAUC at 4 hour follow-up although they were not statistically significant (rho=0.46 and 0.41, P=0.09 and 0.13,

respectively). At other time points including 24 hour, 3 days, and 7 days, no significant correlation was shown between relative changes in IVIM-DWI parameters and those in DCE-MR parameters ($P>0.05$).

Table 8. Correlation in Measured Values at Baseline and 7 Day Follow-up Between Perfusion-related IVIM-DWI Parameters and DCE-MR Parameters (n=21)

Parameters		DCE-MRI			
		K^{trans} (min^{-1})		iAUC (mmol/sec)	
Baseline		Correlation Coefficient‡	P value*	Correlation Coefficient‡	P value*
IVIM-DWI	D^* (x 10^{-3} mm^2/sec)	0.29	0.20	0.23	0.33
	f (%)	-0.22	0.33	-0.19	0.41
	fD^* (x 10^{-3} mm^2/sec)	0.08	0.74	0.02	0.95
7 day follow-up		Correlation Coefficient‡	P value*	Correlation Coefficient‡	P value*
IVIM-DWI	D^* (x 10^{-3} mm^2/sec)	0.02	0.93	0.09	0.69
	f (%)	0.31	0.18	0.31	0.18
	fD^* (x 10^{-3} mm^2/sec)	0.33	0.15	0.37	0.10

Note. – *All data were tested with Spearman rank correlation test. †Significant value, P<0.05. ‡Spearman correlation coefficient (rho).

Figure 9. Graph demonstrating the correlation between relative change of *fD** and relative change in K^{trans} at 4 hour follow-up after CKD-516 treatment. A significant correlation with a rho of 0.54 (P=0.04) is observed.

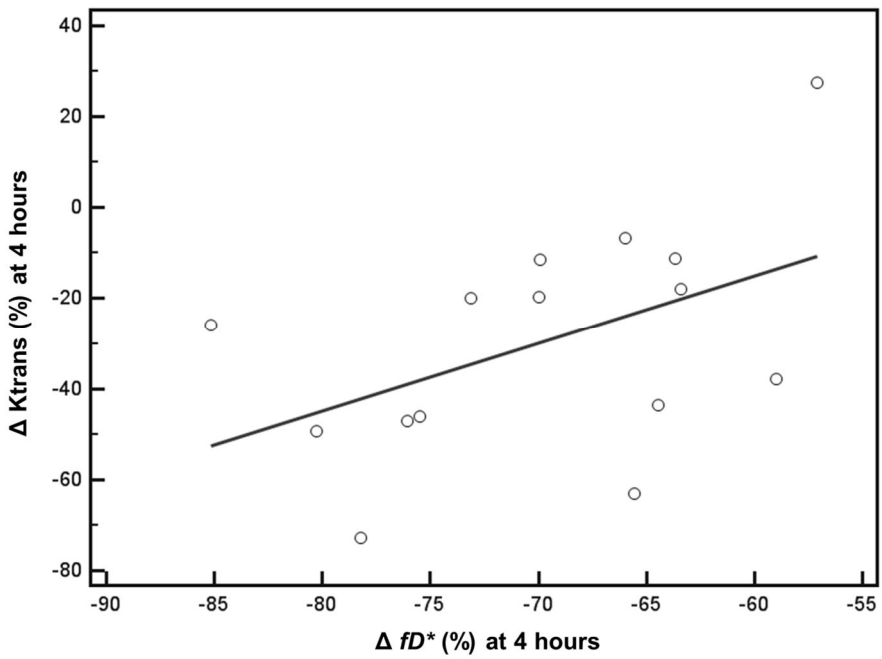

DISCUSSION

This study's results demonstrated that IVIM-DWI and DCE-MRI are able to present serial changes in perfusion and diffusion in rabbit VX2 liver tumor models after administration of CKD-516, with moderate to good reproducibility of the parameters. Among them, relative changes in *f* and fD^* at 4 hours among the DWI parameters can be utilized as early predictors of tumor response. Interestingly, in the CKD-516 treated group, perfusion-related IVIM parameters including D^*, *f,* and fD^*, and DCE-MR parameters including K^{trans} and iAUC decreased at 4 hours and recovered from 24 hours to 3 days, whereas diffusion-related parameters including ADC and *D* increased at 24 hours compared to baseline. The different time courses of change in perfusion and diffusion after VDA treatment can be explained by the intrinsic mechanism of the action of VDAs. As VDAs act by disrupting preexisting tumor blood vessels, its effect on tumor perfusion occurs within hours (10). A decrease in blood flow to the tumor would then result in ischemic changes such as cellular edema and intra-tumoral necrosis, therefore, diffusion-related parameters which reflect the changes in cellularity and necrosis within the tumor (25, 26) would be changed later

than in the perfusion-related parameters. Furthermore, as reproducibility of the measured parameter is one of the essential features for longitudinal studies (27), IVIM-DWI and DCE-MR parameters which show moderate to good reproducibility can be used to monitor the therapeutic effects of anticancer therapy. Based on my observation, I believe that DCE-MRI and IVIM-DWI could be a valuable technique for the evaluation of therapeutic response of VDAs.

In terms of the appropriate timing for imaging studies, my results suggest that IVIM-DWI and DCE-MRI should most optimally be performed within hours after administration of VDA, especially for the evaluation of changes in microscopic perfusion of the target tissue. This study revealed that there were significant differences in ADC at 24 hours, D^* and fD^* at 4 hours, and f, K^{trans} and iAUC at 4 and 24 hours between the control and treated groups ($P<0.05$). However, 3 and 7 days after starting treatment with CKD-516, relative changes in IVIM-DWI and DCE-MR parameters in the treated group were not significantly different from those of the control group ($P>0.05$). In other words, IVIM-DWI and DCE-MR parameters after 3 day follow-up might not be useful for evaluating therapeutic efficacy after CKD-516 treatment. These results are in good agreement with the results of several

previous DCE-MRI studies (28-30), which have demonstrated that perfusion change after VDA administration should be evaluated within hours after starting treatment, whereas perfusion change after anti-angiogenic drug treatment might be assessed even after days and weeks. As VDA's therapeutic effects occur within a few hours after starting treatment, the fact that there was no necessity of contrast medium for IVIM-DWI made it repetitively applicable, which may be a big advantage over DCE-MRI which requires contrast injection for evaluation of the therapeutic effects of VDAs.

Perfusion changes after VDA treatment demonstrated by multiparametric MRI can be explained by their histological changes. My study's results showed that perfusion-related IVIM-DWI parameters *f* and fD^* at 7 day follow-up were significantly correlated with MVD of hot spots within the tumor. As *f* and fD^* is considered to represent blood volume and flow, respectively (31, 32), lower MVD would lead to lower *f* and fD^*, which is consistent with my result at 7 day follow-up. In this study, IVIM-DWI parameters including D^*, *f*, and fD^* and DCE-MR parameters significantly decreased at 4 hours compared to the baseline in the treated group ($P<0.05$). These early perfusion changes were in good agreement with

previous studies which demonstrated that VDAs rapidly collapse the tumor vasculature, resulting in a decrease in velocity (D^*), volume (f), and flow (fD^*) of the blood (32-34). Lavisse et al (8) revealed MVD tended to decrease with time until 24 hours after VDA treatment, which would result in a decrease in *f*. The collapse of preexisting vessels and the decrease in MVD would explain the early changes of perfusion-related parameters within the tumor in the CKD-516 treated group.

After CKD-516 treatment, ADC and *D* decreased at 4 hours and increased at 24 hours compared to baseline. The relative decrease in ADC and *D* at 4 hours compared to baseline can be explained by cellular swelling in acute ischemia and corresponding decrease in volume of extracellular space which reduce the diffusivity of the water (35, 36). Similar to this study's results, Thoeny et al (5) demonstrated that *D* decreased at 1 and 6 hour follow-ups and significantly increased at 2 days, which corresponds to an increase in the necrotic tumor fraction after VDA treatment in rat tumor models. This study's result showing the increase in ADC and *D* at 24 hours can also be explained by the increase in intra-tumoral necrosis considering the significant correlation between the necrotic fraction and diffusion-related parameters including ADC and *D* at 7

days. Experimental studies have shown that VDA would produce a characteristic central necrosis, however, the peripheral viable tumor usually survives and regrows (33), which is consistent with the lower ADC and *D* at 3 days and 7 days than those at 24 days in this study.

This study showed that interval change in *f* and fD^* can be an early predictor for favorable tumor response after CKD-516 treatment. In the CKD-516 treated group, relative changes in *f* and fD^* at 4 hours showed a statistically significant correlation with the final change in tumor size (P=0.04 and 0.009). Relative changes in tumor size during the experimental period of 7 days were significantly lower in the treated group (median of +65.6%) than in the control group (median of +104.6%), which means tumor growth is delayed in the treated group. In this study, I did not follow the classification of RECIST criteria, but instead used interval changes of tumor size in percentages. This was mainly because even in the CKD-516 treated groups, all tumors showed interval growth greater than +20% in diameter, indicating progressive disease. These results were indeed expected as vascular targeting agents are not expected to reduce tumor size in contrast to conventional chemotherapy (37), and VX2 tumors are known to grow aggressively, especially in its early phase (12 to 14 days of

tumor incubation in this study). There have been many studies for the early prediction of tumor response using DCE-MRI in patients treated with vascular targeting agents (38-41), however, there have been few reports detailing the usefulness of IVIM-DWI. Lewin et al (17) revealed that a relative change in *f* would be an early predictor of the treatment efficacy of sorafenib (anti-angiogenic drug) treatment in advanced hepatocellular carcinomas. In terms of VDAs, this study might be the first study to demonstrate the value of *f* and fD^* in predicting a favorable response after treatment of VDA.

In this study, serum TNF-α level markedly increased at 4 hour follow-up in the CKD-516 treated group and recovered at 24 hours. As TNF-α would result in vascular collapse and would increase vascular permeability within the tumor (13), this study's result of serum TNF-α would help explain the early perfusion changes within the tumor after CKD-516 administration. Previous studies have reported that flavonoids (one category of small molecular VDA based on the mechanism of action) can induce high levels of TNF-α by activating tumor-associated macrophages causing up-regulation of mRNA and inducing the secretion of cytokines (42, 43). However, no previous studies have shown that tubulin-binding agents (the

other category of small molecular VDA) would induce TNF-α in vivo. As an example, Kragh et al (44) demonstrated that combretastatin A-4 disodium phosphate (CA4DP), a tubulin-binding agent, does not induce TNF-α production in the tumor. Therefore, further studies would be needed for investigation of the exact action mechanism of TNF-α induction by CKD-516.

In addition, this study's results of correlation analysis between IVIM-DWI parameters and DCE-MR parameters demonstrated no significant correlation between the measured values at baseline and 7 day follow-up, but there was a significant correlation between the relative changes of IVIM-derived fD^* and those of K^{trans} (rho=0.54, P=0.04) at 4 hours after VDA treatment. Based on the basic concept of IVIM-DWI, IVIM measures the motion of blood itself and reflects the perfusion characteristics of the tissue. However, unlike DCE-MRI which would measure classical perfusion determined by the pattern of delivery using tracers, IVIM-DWI cannot measure true perfusion (45). Until now, it has been controversial whether perfusion-related parameters of IVIM-DWI could correlate with DCE-MRI. This study's results would suggest that IVIM-DWI cannot replace DCE-MRI for measuring the perfusion characteristics of the tumors, however, early

perfusion changes measured by DCE-MRI and IVIM-DWI can show correlation after VDA treatment. Similar to this study, Patel et al (46) reported that there was no significant correlation between perfusion-related IVIM-DWI parameters (f and D^*) and DCE-MR parameters for the evaluation of liver cirrhosis. However, there was a study to the contrary, in which Chandarana et al (47) revealed good correlation between IVIM-DWI parameter of f and DCE-MR parameter of iAUC for the vascularity evaluation of renal tumors. In addition, Thoeny et al. showed that $ADC_{perfusion}$ ($=D^*-D$), which is a similar concept to f, would be correlated with DCE-MRI for evaluating the therapeutic effect of VDA in a rat tumor model (5).

This study has several limitations. First, I only evaluated the correlation of IVIM-DWI and DCE-MR parameters with histologic features at 7 day follow-up. Thus, I could not assess early histologic change, which might have explained the early changes in IVIM-DWI and DCE-MR parameters. Second, to measure the multiparametric MR parameters, I selected one ROI in one axial MR image of the tumor at each time point. However, considering the three dimensional structure of the tumor, measurement at cross sectional images might be less representative of the entire tumor

than volumetric measurements. In addition, measurement using one ROI including the whole tumor cannot sufficiently evaluate the pixel-by-pixel change in serial follow-up. Volumetric and pixel-by-pixel quantitative analysis would be superior to the method used in this study for assessment of perfusion and diffusion change in the entire tumor and different regions of the tumor after VDA treatment. Third, this study evaluated the therapeutic efficacy of CKD-516 alone, not in combination with other anticancer treatments. However, currently, VDA alone is not thought to be so effective for tumor control, and a combination of VDA and other conventional therapies may increase the antitumor effect (48). Thus, a combination treatment of VDA and other therapeutic options such as anti-angiogenic drugs, cytotoxic drugs, or radiation treatment would be warranted.

In conclusion, the therapeutic effect induced by CKD-516, a new VDA, can be effectively evaluated with multiparametric MRI including IVIM-DWI and DCE-MRI, and *f* and *fD derived from IVIM-DWI can be utilized as early predictive indicators for tumor response.**

REFERENCES

1. McKeage MJ, Baguley BC. Disrupting established tumor blood vessels: an emerging therapeutic strategy for cancer. Cancer. [Research Support, Non-U.S. Gov't

Review]. 2010 Apr 15;116(8):1859-71.

2. Salmon BA, Salmon HW, Siemann DW. Monitoring the treatment efficacy of the vascular disrupting agent CA4P. Eur J Cancer. [Research Support, N.I.H., Extramural]. 2007 Jul;43(10):1622-9.

3. Delmonte A, Sessa C. AVE8062: a new combretastatin derivative vascular disrupting agent. Expert Opin Investig Drugs. [Review]. 2009 Oct;18(10):1541-8.

4. Padhani AR. Functional MRI for anticancer therapy assessment. Eur J Cancer. [Research Support, Non-U.S. Gov't

Review]. 2002 Nov;38(16):2116-27.

5. Thoeny HC, De Keyzer F, Vandecaveye V, Chen F, Sun X, Bosmans H, et al. Effect of vascular targeting agent in rat tumor model: dynamic contrast-enhanced versus diffusion-weighted MR imaging. Radiology. [Comparative Study

Research Support, Non-U.S. Gov't]. 2005 Nov;237(2):492-9.

6. Thoeny HC, De Keyzer F, Chen F, Ni Y, Landuyt W, Verbeken EK, et al. Diffusion-weighted MR imaging in monitoring the effect of a vascular targeting agent on rhabdomyosarcoma in rats. Radiology. [Research Support, Non-U.S. Gov't]. 2005 Mar;234(3):756-64.

7. Desar IM, ter Voert EG, Hambrock T, van Asten JJ, van Spronsen DJ, Mulders PF, et al. Functional MRI techniques demonstrate early vascular changes in renal cell cancer patients treated with sunitinib: a pilot study. Cancer Imaging. 2011;11:259-65.

8. Lavisse S, Lejeune P, Rouffiac V, Elie N, Bribes E, Demers B, et al. Early quantitative evaluation of a tumor vasculature disruptive agent AVE8062 using dynamic contrast-enhanced ultrasonography. Invest Radiol. 2008 Feb;43(2):100-11.

9. Cyran CC, von Einem JC, Paprottka PM, Schwarz B, Ingrisch M, Dietrich O, et al. Dynamic contrast-enhanced computed tomography imaging biomarkers correlated with immunohistochemistry for monitoring the effects of sorafenib on experimental prostate carcinomas. Invest Radiol. [Evaluation Studies

Research Support, Non-U.S. Gov't

Validation Studies]. 2012 Jan;47(1):49-57.

10. O'Connor JP, Jackson A, Parker GJ, Jayson GC. DCE-MRI biomarkers in the clinical evaluation of antiangiogenic and vascular disrupting agents. Br J Cancer. [Research Support, Non-U.S. Gov't Review]. 2007 Jan 29;96(2):189-95.

11. Chen F, Feng Y, Zheng K, De Keyzer F, Li J, Cona MM, et al. Enhanced antitumor efficacy of a vascular disrupting agent combined with an antiangiogenic in a rat liver tumor model evaluated by multiparametric MRI. PloS one. [Research Support, Non-U.S. Gov't]. 2012;7(7):e41140.

12. Liu G, Rugo HS, Wilding G, McShane TM, Evelhoch JL, Ng C, et al. Dynamic contrast-enhanced magnetic resonance imaging as a pharmacodynamic measure of response after acute dosing of AG-013736, an oral angiogenesis inhibitor, in patients with advanced solid tumors: results from a phase I study. J Clin Oncol. 2005 Aug 20;23(24):5464-73.

13. McPhail LD, McIntyre DJ, Ludwig C, Kestell P, Griffiths JR, Kelland LR, et al. Rat tumor response to the vascular-disrupting agent 5,6-dimethylxanthenone-4-acetic acid as measured by dynamic contrast-enhanced magnetic resonance imaging, plasma 5-hydroxyindoleacetic acid levels, and tumor necrosis. Neoplasia. 2006 Mar;8(3):199-206.

14. Lee J, Kim SJ, Choi H, Kim YH, Lim IT, Yang HM, et al.

Identification of CKD-516: a potent tubulin polymerization inhibitor with marked antitumor activity against murine and human solid tumors. J Med Chem. [Research Support, Non-U.S. Gov't]. 2010 Sep 9;53(17):6337-54.

15. Le Bihan D, Breton E, Lallemand D, Grenier P, Cabanis E, Laval-Jeantet M. MR imaging of intravoxel incoherent motions: application to diffusion and perfusion in neurologic disorders. Radiology. 1986 Nov;161(2):401-7.

16. Koh DM, Collins DJ, Orton MR. Intravoxel incoherent motion in body diffusion-weighted MRI: reality and challenges. AJR Am J Roentgenol. [Research Support, Non-U.S. Gov't

Review]. 2011 Jun;196(6):1351-61.

17. Lewin M, Fartoux L, Vignaud A, Arrive L, Menu Y, Rosmorduc O. The diffusion-weighted imaging perfusion fraction f is a potential marker of sorafenib treatment in advanced hepatocellular carcinoma: a pilot study. Eur Radiol. 2011 Feb;21(2):281-90.

18. Thoeny HC, Ross BD. Predicting and monitoring cancer treatment response with diffusion-weighted MRI. J Magn Reson Imaging. [Research Support, N.I.H., Extramural

Research Support, Non-U.S. Gov't

Review]. 2010 Jul;32(1):2-16.

19. Le Bihan D, Breton E, Lallemand D, Aubin ML, Vignaud J, Laval-Jeantet M. Separation of diffusion and perfusion in intravoxel incoherent motion MR imaging. Radiology. 1988 Aug;168(2):497-505.

20. Mross K, Fasol U, Frost A, Benkelmann R, Kuhlmann J, Buchert M, et al. DCE-MRI assessment of the effect of vandetanib on tumor vasculature in patients with advanced colorectal cancer and liver metastases: a randomized phase I study. J Angiogenes Res. 2009;1:5.

21. Tofts PS, Kermode AG. Measurement of the blood-brain barrier permeability and leakage space using dynamic MR imaging. 1. Fundamental concepts. Magn Reson Med. 1991 Feb;17(2):357-67.

22. Tofts PS, Brix G, Buckley DL, Evelhoch JL, Henderson E, Knopp MV, et al. Estimating kinetic parameters from dynamic contrast-enhanced T(1)-weighted MRI of a diffusable tracer: standardized quantities and symbols. J Magn Reson Imaging. 1999 Sep;10(3):223-32.

23. Poff JA, Allen CT, Traughber B, Colunga A, Xie J, Chen Z, et al. Pulsed high-intensity focused ultrasound enhances apoptosis and growth inhibition of squamous cell carcinoma xenografts with proteasome inhibitor bortezomib. Radiology. 2008 Aug;248(2):485-91.

24. Iellamo F, Legramante JM, Raimondi G, Castrucci F, Massaro M, Peruzzi G. Evaluation of reproducibility of spontaneous baroreflex sensitivity at rest and during laboratory tests. Journal of hypertension. [Research Support, Non-U.S. Gov't]. 1996 Sep;14(9):1099-104.

25. Koh DM, Collins DJ. Diffusion-weighted MRI in the body: applications and challenges in oncology. AJR Am J Roentgenol. 2007 Jun;188(6):1622-35.

26. Thoeny HC, De Keyzer F. Extracranial applications of diffusion-weighted magnetic resonance imaging. Eur Radiol. 2007 Jun;17(6):1385-93.

27. Jackson A, Jayson GC, Li KL, Zhu XP, Checkley DR, Tessier JJ, et al. Reproducibility of quantitative dynamic contrast-enhanced MRI in newly presenting glioma. Br J Radiol. 2003 Mar;76(903):153-62.

28. Ricart AD, Ashton EA, Cooney MM, Sarantopoulos J, Brell JM, Feldman MA, et al. A phase I study of MN-029 (denibulin), a novel vascular-disrupting agent, in patients with advanced solid tumors. Cancer chemotherapy and pharmacology. 2011 Oct;68(4):959-70.

29. Salmon HW, Siemann DW. Effect of the second-generation vascular disrupting agent OXi4503 on tumor vascularity. Clinical cancer

research : an official journal of the American Association for Cancer Research. 2006 Jul 1;12(13):4090-4.

30. Stevenson JP, Rosen M, Sun W, Gallagher M, Haller DG, Vaughn D, et al. Phase I trial of the antivascular agent combretastatin A4 phosphate on a 5-day schedule to patients with cancer: magnetic resonance imaging evidence for altered tumor blood flow. J Clin Oncol. 2003 Dec 1;21(23):4428-38.

31. Sigmund EE, Vivier PH, Sui D, Lamparello NA, Tantillo K, Mikheev A, et al. Intravoxel incoherent motion and diffusion-tensor imaging in renal tissue under hydration and furosemide flow challenges. Radiology. 2012 Jun;263(3):758-69.

32. Federau C, Maeder P, O'Brien K, Browaeys P, Meuli R, Hagmann P. Quantitative Measurement of Brain Perfusion with Intravoxel Incoherent Motion MR Imaging. Radiology. 2012 Dec;265(3):874-81.

33. Thorpe PE. Vascular targeting agents as cancer therapeutics. Clinical cancer research : an official journal of the American Association for Cancer Research. 2004 Jan 15;10(2):415-27.

34. Griggs J, Metcalfe JC, Hesketh R. Targeting tumour vasculature: the development of combretastatin A4. Lancet Oncol. 2001 Feb;2(2):82-7.

35. Doczi T, Schwarcz A. Correlation of apparent diffusion coefficient and computed tomography density in acute ischemic stroke. Stroke. 2003 May;34(5):e17-8; author reply e-8.

36. Wang H, Marchal G, Ni Y. Multiparametric MRI biomarkers for measuring vascular disrupting effect on cancer. World J Radiol. 2011 Jan 28;3(1):1-16.

37. Siemann DW, Mercer E, Lepler S, Rojiani AM. Vascular targeting agents enhance chemotherapeutic agent activities in solid tumor therapy. International journal of cancer Journal international du cancer. 2002 May 1;99(1):1-6.

38. Hsu CY, Shen YC, Yu CW, Hsu C, Hu FC, Hsu CH, et al. Dynamic contrast-enhanced magnetic resonance imaging biomarkers predict survival and response in hepatocellular carcinoma patients treated with sorafenib and metronomic tegafur/uracil. J Hepatol. 2011 Oct;55(4):858-65.

39. Chang YC, Yu CJ, Chen CM, Hu FC, Hsu HH, Tseng WY, et al. Dynamic contrast-enhanced MRI in advanced nonsmall-cell lung cancer patients treated with first-line bevacizumab, gemcitabine, and cisplatin. J Magn Reson Imaging. 2012 Aug;36(2):387-96.

40. Hirashima Y, Yamada Y, Tateishi U, Kato K, Miyake M, Horita Y, et

al. Pharmacokinetic parameters from 3-Tesla DCE-MRI as surrogate biomarkers of antitumor effects of bevacizumab plus FOLFIRI in colorectal cancer with liver metastasis. International journal of cancer Journal international du cancer. 2012 May 15;130(10):2359-65.

41. Akisik MF, Sandrasegaran K, Bu G, Lin C, Hutchins GD, Chiorean EG. Pancreatic cancer: utility of dynamic contrast-enhanced MR imaging in assessment of antiangiogenic therapy. Radiology. 2010 Aug;256(2):441-9.

42. Jassar AS, Suzuki E, Kapoor V, Sun J, Silverberg MB, Cheung L, et al. Activation of tumor-associated macrophages by the vascular disrupting agent 5,6-dimethylxanthenone-4-acetic acid induces an effective CD8+ T-cell-mediated antitumor immune response in murine models of lung cancer and mesothelioma. Cancer research. [Research Support, N.I.H., Extramural]. 2005 Dec 15;65(24):11752-61.

43. Hasani A, Leighl N. Classification and toxicities of vascular disrupting agents. Clinical lung cancer. [Review]. 2011 Jan;12(1):18-25.

44. Kragh M, Quistorff B, Horsman MR, Kristjansen PE. Acute effects of vascular modifying agents in solid tumors assessed by noninvasive laser Doppler flowmetry and near infrared spectroscopy. Neoplasia. [Research Support, Non-U.S. Gov't]. 2002 May-Jun;4(3):263-7.

45. Henkelman RM. Does IVIM measure classical perfusion? Magn Reson Med. 1990 Dec;16(3):470-5.

46. Patel J, Sigmund EE, Rusinek H, Oei M, Babb JS, Taouli B. Diagnosis of cirrhosis with intravoxel incoherent motion diffusion MRI and dynamic contrast-enhanced MRI alone and in combination: preliminary experience. J Magn Reson Imaging. 2010 Mar;31(3):589-600.

47. Chandarana H, Kang SK, Wong S, Rusinek H, Zhang JL, Arizono S, et al. Diffusion-weighted intravoxel incoherent motion imaging of renal tumors with histopathologic correlation. Invest Radiol. 2012 Dec;47(12):688-96.

48. Horsman MR, Siemann DW. Pathophysiologic effects of vascular-targeting agents and the implications for combination with conventional therapies. Cancer research. 2006 Dec 15;66(24):11520-39.

초 록

서론: 복셀내 비결집 운동 (intravoxel incoherent motion, IVIM) 확산 강조 영상과 역동적 조영 증강 영상을 포함한 다중지표 자기공명영상(Multiparametric MRI)이 혈관차단제(CKD-516)의 치료 효과를 정량적으로 평가하는데 유용한 진단 도구인지 토끼 VX2 간암 모델을 이용하여 평가하고자 한다.

방법: VX2 간암 모델 토끼 21 마리(15 마리의 치료군과 6 마리의 대조군)를 제작한 후 CKD-516 투약 전, 투약 후 4 시간, 24 시간, 3 일, 7 일에 3T MRI 스캐너로 12 개의 b 값을 이용한 IVIM 확산 강조 영상과 역동적 조영 증강 영상을 촬영하였다. 간 종양의 IVIM 확산 강조 영상 지표로는 apparent diffusion coefficient (ADC), true diffusion coefficient (D), pseudo-diffusion coefficient (D^*), perfusion fraction (f), blood flow-related parameter (fD^*)를 얻었고 역동적 조영 증강 영상 지표로는 volume transfer coefficient (K^{trans})와 initial area under the gadolinium concentration-time curve until 60 seconds (iAUC)을 측정하였다. 대조군과 치료군에서 IVIM 확산 강조

영상 지표와 역동적 조영 증강 영상 지표를 비교하였으며 치료군에서 각 지표의 시간대 별 측정치를 비교하였다. CKD-516 치료에 대한 종양 반응을 예측할 수 있는 인자를 찾기 위해 IVIM 확산 강조 영상 지표와 역동적 조영 증강 영상 지표와 종양 크기 변화 사이의 상관 관계를 분석하였다. 또한 IVIM 확산 강조 영상 지표와 역동적 조영 증강 영상 지표 사이에 상관 관계가 있는지 분석하였다.

결과: 치료군은 대조군과 비교하여 24 시간에 ADC 값이 유의하게 증가하였으며 4 시간에 D^*와 fD^*가 감소하였고 4 시간과 24 시간에 f, K^{trans}, iAUC 값이 감소하였다 (P<0.05). 치료군에서 시간대별 측정치를 baseline 과 비교하였을 때 D^*, f, fD^*, K^{trans}, iAUC 가 4 시간에 유의하게 감소한 후 24 시간에서 3 일에 거쳐 회복되었고 D는 24 시간에 유의하게 증가하였다 (P<0.005). 또한 4 시간에 f와 fD^*가 많이 감소할수록 7 일 동안 종양 크기가 적게 증가하였다 (각각 rho=0.53 과 0.65, P=0.04 와 0.009). IVIM 확산 강조 영상 지표와 역동적 조영 증강 영상 지표간의 상관 관계를 분석하였을 때 측정치 간에는 유의한 상관 관계가 없었으나 (P>0.05) 4 시간 추적 영상에서

baseline 과 비교하여 fD^*와 K^{trans}의 상대적 변화 정도 사이에 유의한 양성 상관 관계가 관찰되었다 (rho=0.54, P=0.04).

결론: 혈관차단제에 의한 치료 효과는 IVIM 확산 강조 영상과 역동적 조영 증강 자기 공명 영상을 이용하여 효과적으로 평가가 가능하며 IVIM 확산 강조 영상 지표 중 f와 fD^*는 종양 반응 평가의 조기 예측 인자로 사용할 수 있었다.

주요어: 복셀내 비결집 운동 확산 강조 자기 공명 영상, 역동적 조영 증강 자기 공명 영상, 혈관차단제, CKD-516, 간암, VX2 종양

학번: 2011-30580